Are low- and high-loss glass–ceramic optical fibers possible game changers?

Wilfried Blanc, Daniele Tosi, Arnaldo Leal-Junior, Maurizio Ferrari, John Ballato

▶ **To cite this version:**

Wilfried Blanc, Daniele Tosi, Arnaldo Leal-Junior, Maurizio Ferrari, John Ballato. Are low- and high-loss glass–ceramic optical fibers possible game changers?. Optics Communications, 2025, 575, pp.131300. 10.1016/j.optcom.2024.131300 . hal-05160041

HAL Id: hal-05160041
https://hal.science/hal-05160041v1

Submitted on 12 Jul 2025

HAL is a multi-disciplinary open access archive for the deposit and dissemination of scientific research documents, whether they are published or not. The documents may come from teaching and research institutions in France or abroad, or from public or private research centers.

L'archive ouverte pluridisciplinaire **HAL**, est destinée au dépôt et à la diffusion de documents scientifiques de niveau recherche, publiés ou non, émanant des établissements d'enseignement et de recherche français ou étrangers, des laboratoires publics ou privés.

Are low- and high-loss glass–ceramic optical fibers possible game changers?

Wilfried Blanc [a,*], Daniele Tosi [b,c], Arnaldo Leal-Junior [d], Maurizio Ferrari [e], John Ballato [f]

[a] Université Côte d'Azur, CNRS, INPHYNI, France
[b] Nazarbayev University, School of Engineering and Digital Sciences, 53 Kabanbay Batyr, 010000, Astana, Kazakhstan
[c] National Laboratory Astana, Laboratory of Biosensors and Bioinstruments, 53 Kabanbay Batyr, 010000, Astana, Kazakhstan
[d] Federal University of Espírito Santo, Fernando Ferrari Avenue, 29075-910, Vitória, Brazil
[e] IFN-CNR CSMFO Lab. and FBK Photonics Unit, Via alla Cascata 56/C Povo, 38123, Trento, Italy
[f] Department of Materials Science and Engineering, Clemson University, Clemson, SC, 29634, USA

ARTICLE INFO

Keywords:
Optical fiber
Silica
Nanoparticles
Lasers
Sensors

ABSTRACT

The transparency of optical fibers is one of the most sought-after properties for this optical waveguide, the paradigmatic example being fibers for long-haul telecommunications. This transparency is achieved by eliminating absorbing centers and heterogeneities. So, the idea of deliberately introducing nanoparticles into the core of a fiber seems to go against the usual doxa, given the light scattering they induce. Such fibers, mainly based on silica glass, were first designed to modify luminescence properties to develop fiber lasers and amplifiers. For such applications, light scattering must be limited. However, over the last five years, light scattering has proved to be a valuable property for sensor applications. This review article is an opportunity to review the state of the art in nanoparticle-containing optical fibers, and to highlight their potential for laser and sensor applications.

1. Introduction

Following the seminal article written by C.K. Kao and G. Hockham in 1966, the enormous potential of the optical telecommunications market led to an unprecedented drive to produce such transparent optical fiber [1]. Thanks to new manufacturing processes, the ability to transmit 1% of the initial power was increased from 20 m to 100 km during the 1970s, paving the way for long-haul telecommunication. Fueled by this success, optical fibers have since expanded to other applications such as amplifiers, lasers, sensors - all fields in which Sir David Payne, whom we celebrate in this special issue, was a pioneer. Examples include his seminal work on the erbium-doped fiber amplifiers which paved the way for the Internet, high-power fiber lasers which have a huge impact in industry for materials processing, drilling, cutting, etc., and the solution doping technique which has extended the composition range for silica-based fibers [2–4].

In the face of such success, the question is no longer whether optical fibers are interesting, but rather what their limits are. To push back these limits, the initial optical fiber, based on silica glass and core-cladding structure, has evolved into a multitude of optical fibers made of different materials (fluoride, chalcogenide, multimaterials, etc.) or structures (photonic crystal fiber, microstructured fiber, D-shaped, etc.) [5]. Thanks to the revolution brought about by and for optical fibers, they have been elected one of the 7 Wonders of the Glass World at the end of the International Year of Glass in 2022 [6].

Since fiber is used to guide light, the main paradigm driving its development is the quest for transparency. The leitmotiv of manufacturing processes was to eliminate the presence of absorbing centers such as iron, and to limit heterogeneity in composition and structure. Recent advances in ultra-low loss fiber are a perfect example of this, with a silica-only core (to limit compositional fluctuations compared with conventional germanium-doped cores) and very precise control of thermal profiles during drawing to promote structural relaxation of the glass (thus reducing structural heterogeneity) [7].

In this context, the idea of introducing heterogeneity such as nanoparticles into optical fibers may seem like an oxymoron, since optical fibers are supposed to guide light, while nanoparticles scatter it. Perhaps unsurprising is that fact that nanostructured glasses, though not yet fibers, were being considered as early as at least the 1970s [8] as the first low loss optical fibers were being fabricated and the field of photonics was nascent but well appreciated for its potential [9]. Those "vitro--ceramics," with compositions in the GeO_2-PbF_2 system (co-doped with Er/Yb and Yb/Tm), nucleated and grew fluoride nanocrystalline phases inside the oxide glass and led to observed infrared upconversion from the rare earth dopants that partitioned into the low vibrational energy (crystalline) fluoride phase. Glass-ceramic fibers enter the picture in the

late 1980s/early 1990s when global attention was focused on high temperature superconductivity [10,11].

As photonics and fiber optics continued to evolve, the development of new materials for these emerging fields gained attention, and such oxyfluoride glass-ceramics returned to the fore, also relating to wavelength conversion [12]. The transition from bulk glass-ceramics to fibers or, more specifically to waveguides, comes in 1998 when *Tick* poses the question "Are low-loss glass–ceramic optical waveguides possible?" [13].

This review aims to extend this question to its opposite, to demonstrate that it is not only a question of low-loss but high-loss offers unique opportunity too. In the first part, we will discuss the influence of different nanoparticle characteristics (size, composition, structure, etc.) in relation to light scattering and in modifying the luminescence properties of rare-earth ions and transition metals. This is followed by a presentation of the various approaches to fabricating such fibers. The following paragraphs are devoted to applications. First, we'll discuss how lasers can be made from such fibers. Then, sensors will be presented. These take advantage of light scattering, and two analysis methods will be discussed, one based on the analysis of backscattered light using Optical Backscatter reflectometry, the other relies on Transmission-Reflection Analysis. Such sensors can be used to measure various parameters such as temperature, mechanical deformation, changes in the biological or chemical environment, etc.

2. Draw me a nanoparticle

In relation to the applications described in the next parts of this article, two functions are sought for nanoparticles: (i) light scattering and (ii) modification of luminescence properties. In this section, we will briefly describe how the characteristics (size, size distribution, shape, density, composition and structure) of the nanoparticles can impact these two functions.

2.1. Light scattering

To give general comments on the effects of nanoparticle characteristics on light scattering, we first use the model developed by Lord Rayleigh. It assumes that nanoparticles are much smaller (>10x) than the wavelength, which is verified, for example, for particles smaller than 100 nm and a wavelength of 1.5 µm. The effective Rayleigh scattering cross-section of a particle is given by:

$$C_{Rayleigh} = \frac{(2\pi)^5}{48}\frac{d^6}{\lambda^4}n_m^4\left(\frac{n_n^2 - n_m^2}{n_n^2 + 2n_m^2}\right)^2 \quad (1)$$

where d corresponds to the particle diameter, λ to the wavelength, n_m and n_n to the refractive indices of the glass matrix and the nanoparticle, respectively [14]. Now, we discuss the effect of the different characteristics of the nanoparticles on light scattering. In particular, we will focus on the operating wavelength, the refractive index, the size and the volume fraction.

- **Operating wavelength.** According to this formula, the operating wavelength could be an important criterion, since the effective absorption cross-section varies to the 4^{th} power of this parameter. Increasing (resp. decreasing) the wavelength would decrease (resp. increase) the light scattering. However, operating wavelengths are usually restricted to a limited range imposed by the applications.
- **Refractive index difference.** The refractive index of the particles, or more precisely the refractive index difference with the matrix, is an important criterion to consider. Depending on the nanoparticles under consideration, the refractive index difference can vary from 10^{-3} to 2 (e.g. silicon nanoparticles in silica). Even a small variation of the refractive index of the nanoparticle can have an important impact on the light scattering. Indeed, when the refractive index difference increases from 10^{-3} to 10^{-2}, the effective Rayleigh scattering cross-section is multiplied by 100, and by 10,000 when the index difference increases to 10^{-1}, which may be the case with fluoride nanoparticles such as LaF_3 or lanthanum silicates used for the applications described below. This refractive index difference can be adjusted too by choosing the composition of the glassy matrix. However, by modifying the composition of the core glass, it is necessary to adapt the composition of the cladding glass to match their thermomechanical properties.
- **Refractive index dispersion.** As nanoparticles and matrix have different compositions, their refractive indices have different dispersion relationships. Light scattering can then be minimized at wavelengths where the two materials have very close, or even identical, refractive indices, but this approach is limited to a restricted range of wavelengths [15].
- **Birefringence.** A final refractive index effect is caused by birefringence in crystals without a cubic phase. Such effects have been considered in ceramics containing 0.5 µm Al_2O_3 grains [16]. It was then shown that, given the random orientation of the birefringent grains, the refractive index difference between the matrix and the crystallites could be considered as $(2/3)\Delta n_{max}$, where Δn_{max} corresponds to the refractive index difference between the ordinary and extraordinary axes.
- **Nanoparticle size.** Nanoparticle size is a particularly important criterion, as the effective scattering cross-section depends to the power of 6 on this parameter (Rayleigh approach), and manufacturing processes allow particle size to vary over several orders of magnitude, from nm to µm and beyond. This explains why particular attention is paid to size among the various characteristics. In addition to affecting the effective cross-section of light scattering, nanoparticle size also modifies the angular distribution of scattered light. In the case of Rayleigh scattering, light is scattered forwards and backwards equally, with less scattering to the side. As particle size increases (nanoparticle size comparable to the wavelength, Mie scattering regime), light is mainly scattered forwards, to the detriment of light backscattering. Similarly, as particles grow in size, their shape becomes more important for scattering property [17]. For instance, there is less backscattered light for prolate particles compared to equivalent spherical particle [14].
- **Volume fraction.** Assuming a low volume fraction, nanoparticles can be considered independent, and the scattered light corresponds to the effective scattering cross-section multiplied by the number of particles. However, in the case of small monodisperse nanoparticles, this linear variation is limited up to a volume fraction of the order of 10%. Above this value, optical interference effects lead to an increase in the signal transmitted through the medium containing the nanoparticles compared to the intensity estimated with the Rayleigh model [18].

As we are interested in optical fibers in this article, the structure of this waveguide must also be considered to evaluate the light scattering property. Indeed, light is guided in the fiber core according to different transverse modes of propagation that are axisymmetric with respect to the fiber axis, but they are not completely confined within the core. Part of the mode lies outside the core, *i.e.* in the cladding. Depending on the opto-geometric structure of the fiber (core radius and refractive index difference between core and cladding), each mode has a certain overlap factor with the core, and therefore interacts with the nanoparticles. In the case of a single-mode fiber, this overlap factor is typically of the order of 80% at 1.5 µm for the fundamental mode (approximated by a Gaussian) and increases with decreasing wavelength or decreases, at a given wavelength, for higher-order modes if the fiber is multimode [19]. Therefore, the effective Rayleigh scattering cross-section must be multiplied by an overlap factor, specific to each propagation mode. Given this extension of transverse propagation modes outside of the core, nanoparticles can also be placed in a ring around the core to adjust

light scattering property [20].

The light scattered by nanoparticles is distributed in all directions in space, unlike reflectors such as Bragg gratings, which reflect backwards only. Only a fraction of the light scattered by nanoparticles is therefore trapped in the core and guided backward and forward. This fraction of light depends on the numerical aperture (NA) of the fiber, $NA=(n_1^2-n_2^2)^{1/2}$ where n_1 and n_2 are the refractive index of the core and the cladding, respectively. The fraction of scattered light which is trapped in the core is determined by the recapture coefficient S defined by:

$$S=\frac{3/2}{\left(\frac{\omega_0}{a}\right)^2 V^2}\frac{n_1^2-n_2^2}{n_1^2} \tag{2}$$

where w_0 is the mode field diameter, a is the core radius, V is the normalized frequency, n_1 and n_2 are the refractive indices of the core and cladding, respectively [21]. In the case of a single-mode fiber ($1.5 \leq V \leq 2.4$), the recapture coefficient varies between:

$$0.21\frac{n_1^2-n_2^2}{n_1^2} \leq S \leq 0.235\frac{n_1^2-n_2^2}{n_1^2} \tag{3}$$

For an SMF28 fiber, $(n_1^2-n_2^2)/n_1^2 = 0.007$, then S is about 0.1%. This value of S can be increased by increasing the core refractive index, but this also changes the guiding properties, and the single-mode fiber can become multimode. For such fibers, the recapture coefficient term for step index fibers is [22,23]:

$$S_{step} = 0.38\frac{NA^2}{n_1^2} \tag{4}$$

and for gradient-index fibers:

$$S_{graded} = 0.25\frac{NA^2}{n_1^2} \tag{5}$$

The recapture coefficient can be used to estimate the backscattered power P_{bs}:

$$P_{bs}(z) = P_{in}\left(\frac{v_g W}{2}\right)\alpha_R S \exp(-2\alpha z) \tag{6}$$

where α_R is the attenuation constant caused by light scattering, W is the temporal pulse width, P_{in} is the incident power, α is the total absorption coefficient (including α_s), v_g is the group velocity. If we consider $Vg = 2.10^8$ m/s, W = 1 ns, $\alpha_S \approx \alpha = 0.2$ dB/km ($4.6.10^{-5}$ m^{-1}) at 1.5 μm, S = 0.0015, then the Rayleigh backscattered signal power is −81 dB/m. An increase in the scattering coefficient α_R increases the backscattered power, thus improving the signal-to-noise ratio. However, increasing α_R also leads to a faster decrease in power along the fiber. A compromise must therefore be found in relation to the intended application. In order to quantify this compromise, a quality factor has been proposed [24]:

$$Q_{enh} = 10\log_{10}(\eta_{enh}) - 2L(\alpha_M - \alpha_{SMF28}) \tag{7}$$

where η_{enh} is the ratio of the backscattering coefficients of NP-doped fiber and SMF28, and α_M and α_{SMF28} are the attenuation coefficients of the NP-doped fiber and SMF28, respectively. In the right part of the equation, the first member relates to the positive effect brought about by the increase in light scattering, counterbalanced by the negative effect linked to the increase in attenuation as described in the second member. It is then possible to define a length L_{enh} (corresponding to $Q_{enh} = 0$) above which the gain from increased Rayleigh scattering is offset by increased attenuation losses:

$$L_{enh} = \frac{10\log_{10}(\eta_{enh})}{2(\alpha_M - \alpha_{SMF28})} \tag{8}$$

2.2. Luminescence engineering

The laser and amplifier applications discussed in the next section of this article rely on the spectroscopic properties of luminescent ions (rare-earth or transition metal ions). These properties depend on the chemical and structural environment of the luminescent ions [25]. However, composition of interest for luminescence properties may not be drawn into fiber. Nanoparticles of this composition can then be an alternative when inserted in a glass such as silica which is commonly used to prepare optical fibers. Nanoparticles can therefore allow to obtain new luminescence properties, which could not be reached with the silica environment. In this luminescence context dealing with fiber lasers and amplifiers, light scattering induced by nanoparticles must be minimized. The effects of the nanoparticles characteristics on luminescence property of rare-earth ions are now presented. First we will discuss on the effect of the structure (crystalline or amorphous) and the composition. Such alterations are known for bulk materials. The last effect, related to the size, is specific to the nanoparticles and highlights the importance of the surrounding material.

- **Crystal/amorphous.** A crystalline nanoparticle structure is sought for transition metals, as they have very low emission efficiencies in an amorphous environment [26]. For rare-earth ions, a crystalline structure has the advantage over an amorphous environment of higher absorption and emission cross sections, but at the expense of absorption and emission bandwidths. Amorphous nanoparticles can lead to a broadening of the emission spectrum of rare-earth ions, such as the emission band at 1.55 μm of Er^{3+}, which is of interest for amplification applications [27].
- **Composition.** As far as composition is concerned, fluoride nanoparticles are of interest because they have a lower phonon energy than silica. This increases the rate of radiative de-excitations relative to the rate of non-radiative de-excitations, improving the quantum efficiency (and the fluorescence lifetime) of certain transitions for rare-earth ions [28]. Phonon energy should also be considered when non-resonant energy transfer between luminescent ions is involved in the excitation process and. Phosphate-based nanoparticles are matrices that allow higher rare-earth ions doping than silica, before achieving luminescence quenching by concentration [29]. Nanoparticles enabling high concentrations of rare-earth ions to be achieved are important because, since nanoparticles only represent a volume fraction of 1–10%, this means that for the same average concentration as in a conventional fiber, the concentration in the nanoparticles must be multiplied by 10 or 100.
- **Size effect.** The choice of nanoparticles could be based on the known luminescence properties of the bulk material. However, downscaling to the nanoscale can lead to differences. Some nanoparticles are obtained by phase separation mechanisms as described in the next section. It has been shown that with this approach, nanoparticle composition can evolve as a function of nanoparticle size [30]. They become enriched with phase-separating elements as they grow. As a result, the smallest nanoparticles are only slightly modified in composition compared with the glass matrix and are therefore of no interest in luminescence modification. A compromise must therefore be found between a sufficient size to modify luminescence properties while maintaining minimal light scattering. Size-dependent compositional modification also means that the refractive index must evolve with nanoparticle size. This effect is not taken into account, for example, in the Rayleigh approximation, for which a single refractive index exists for nanoparticles regardless of their size. Beyond compositional variation, other size-related effects have been reported. In the case of nanoparticles, it has been shown that the phonon density of state (PDOS) evolves as a function of size. For Y_2O_2S nanocrystals, a confinement effect is manifested by a discretization of the PDOS and the appearance of an acoustic phonon cutoff frequency estimated at 8 and 2 cm^{-1} for nanoparticles with

radius of 5 and 20 nm, respectively [31]. These modifications can impact thermalization processes but remain limited to very low temperatures (<10 K) [32]. When nanoparticles are embedded in a glass matrix, this can also impact the spectroscopic properties of the luminescent ions embedded into the nanoparticles. For example, it has been reported that an increase in the refractive index (from n = 1 to 2.2) of the surrounding matrix contributes to decreasing by a factor of 3 the radiative lifetime of the $^5D_0$ multiplet of the Eu^{3+} ion inserted in a Y_2O_3 nanocrystal (~7 nm) [33]. Finally, in studies involving Ho- or Er-doped LaF_3 nanocrystals (10–20 nm), it was reported that changes in luminescence properties were explained by an interaction between the electronic states of the rare-earth ions present in the nanocrystals and the vibrational modes of the surrounding glass matrix [34,35].

3. Formation of dielectric nanoparticles in optical fiber

To obtain optical fibers with the targeted characteristics of dielectric nanoparticles (the most reported in the literature), two main approaches have been studied to date. The first one is based on *in-situ* formation of nanoparticles induced by thermodynamics mechanisms (phase separation and nucleation/growth), taking advantage of the heat treatment inherent to the manufacturing process or by applying an additional post heat-treatment to the fiber. The second route of interest concerns the direct insertion of the targeted nanoparticles into the glass. In this section, we will also discuss the effect of the drawing step.

3.1. *In-situ formation of nanoparticles*

The approach based on the formation of nanoparticles during the manufacturing process was historically the first one to be used and is still widely used today. This process relies on the ability of glass (for certain composition) to devitrify when submitted to high temperatures. The glass, initially homogeneous, then forms two phases of different compositions. This formation is described by the thermodynamic mechanisms of phase separation or nucleation/growth which are described in detail in Ref. [36].

Such thermodynamics mechanisms have been applied at various stages in the manufacture of optical fibers. The first optical fibers containing nanoparticles were obtained by directly heating the initially homogeneous fiber [26]. With the right choice of heat treatment (temperature, duration), it is thus possible to control the formation and density of the first nuclei, which can then grow to form nanocrystals whose size again depends on the temperature and duration of the heat treatment. This process is identical to that used to form glass ceramics. Generally, in the case of optical fibers, a single temperature is chosen, slightly higher than the glass transition temperature (Tg), to achieve a compromise between nuclei formation and growth. The duration of heat treatment is typically of the order of 1–10 h. This approach is the most used to grow nanocrystals, oxide and fluoride ones, to modify the luminescence properties of rare-earth ions or transition metals [37]. Additionally, this approach can be applied to any glass optical fiber. However, it has some limitations. The polymer coating must be removed from the fiber prior to heat treatment, and then replaced. The length of heat-treated fiber is limited. Finally, heating the fiber can lead to a reduction in its mechanical properties, making it more brittle. The pros and cons of the different approach are highlighted in Table 1.

Thermodynamics mechanisms have also been exploited to obtain nanoparticles directly during the fabrication process. This approach means that hundreds of meters of optical fibers already containing nanoparticles can be obtained directly at the end of the process, without the need for post-thermal treatment of the fiber. This approach has mainly been applied to the manufacture of preforms using the industrial Modified Chemical Vapor Deposition (MCVD) process [27]. This is based on the vapor deposition of a porous silicate layer (typically silica doped with germanium) inside a silica tube. During the solution doping step, ions such as alkaline earths can be dispersed in the porous layer. The next steps involve the sintering of this porous layer and the collapsing of the tube to form a preform. Given the glass is silica, high temperature is required, typically up to 2000–2200 °C during the collapsing stage. At this high temperature, silica glass containing alkaline earth ions demixes to form alkaline earth-rich particles, while the matrix is silica-rich. The process is described here with alkaline earth ions but it can be extended to any ion leading to a phase separation of silica glass. The nanoparticles thus obtained in the preform are usually silicates (silica + phase-separating elements) whose average size depends on the concentration of phase-separating element ions in the doping solution [37]. However, the size distribution can be large, and it is difficult to control it. *In-situ* formation can be applied for luminescence applications since it has been shown that rare earth ions migrate into the nanoparticles and can therefore benefit from the modified chemical and structural environment provided by the nanoparticles [30].

Table 1
Advantages and drawbacks of the different processes used to prepare optical fibers containing nanoparticles.

Process	Pros	Cons
Heating the fiber	- Can be applied to any glass - Accurate control of the NCs size - Fluoride NCs can be obtained	- Limited fiber length - Fiber must be uncoated and recoated - Heating may fragilize the fiber
Along the process	- Based on an industrial process (MCVD) - "infinite" fiber length	- Difficulty to control NPs size distribution - Restricted to phase-separated composition
NP-doping	- Control of the NPs characteristics - Control of the luminescent ions concentration	- High risk of reactivity of the NPs with the glassy matrix - Handling of NPs

3.2. *Embedding nanoparticles*

Why make things complicated when you can make them simple? Since the characteristics of nanoparticles can be identified *a priori*, why not embeding them directly into the glass? Direct doping with nanoparticles seems the most obvious solution, but nanoparticles are subjected to such high constraints during manufacture that it is difficult to maintain their integrity. It has been reported that during the MCVD process, when $YbPO_4$ crystallites are dispersed in the doping solution, such crystallites are observed in the preform and in the fiber [38]. However, the survival of nanocrystals remains largely unreported. In general, nanocrystals react with the silica matrix. For example, Al_2O_3 nanoparticles have been among the most widely used nanocrystals. After preform fabrication, the nanoparticles, smaller in size (~15 nm) than the initial nanocrystals (~50 nm), are partially crystallized and have evolved into a mullite-type silicate ($3Al_2O_3$–$2SiO_2$). In the fiber, these nanoparticles are amorphous [39]. A study of the reactivity of fluoride nanoparticles shows that fluorine evaporates in the form of SiF_4 as soon as the MCVD porous layer is dried. The nanoparticles observed are then silicates [40,41]. Not all nanoparticle transformations lead to silicates. For example, it has been reported that doping with $Y_3Al_5O_{12}$ (YAG) nanocrystals leads to the formation of YPO_4 nanocrystals in the fiber, the phosphorus being present in the porous layer during the MCVD process [42]. Without phoshphorus, YAG nanocrystals transform into amorphous YAS (Y_2O_3–Al_2O_3–SiO_2) nanoparticles [43]. These examples show that although the characteristics of the initial nanocrystals are perfectly determined, it is essential to characterize the nanoparticles in the fibers because their characteristics can evolve. In the case of crystalline nanoparticles, characterization can be performed using both X-ray Diffraction (XRD) and Selected Area Electron Diffraction (SAED). Combined with chemical analysis by Energy Dispersive X-ray (EDX) performed on a thinned slide (typically a slide prepared for TEM

analysis) to improve spatial resolution, these analyses can be used to define the crystalline phase present in the form of nanoparticles. In the case of amorphous particles, such as those obtained via the MCVD process, characterization requires other techniques. The main difficulty lies in characterizing nanoparticles whose composition is close to that of the surrounding matrix. In this context, characterization by Atom Probe Tomography is of major interest, since it takes advantage of the sub-nm spatial resolution of this technique to reconstruct in 3D the distribution of chemical species distributed in the analyzed volume [30].

3.3. Influence of the drawing step

Given the presence of nanoparticles, the drawing step cannot be considered as a simple homothetic transformation of the preform into an optical fiber. Indeed, the particles, which are spherical in the preform, may elongate, or even fragment into daughter particles, aligned along the drawing axis [44]. These changes can be explained by considering the rheology of glass. When a two-phase system is subjected to a deformation such as elongation, the particle shape depends on the capillary number Ca:

$$Ca = \frac{viscous forces}{surface tension} = \frac{\eta R \dot{\varepsilon}}{\gamma} \quad (9)$$

where η is the viscosity, ε is the deformation rate, R_{NP} is the particle radius and γ is the surface tension between the particle and the surrounding liquid. The capillary number highlights the competition between the viscous flow, which tends to elongate the particle, and surface tension, which tends to keep the particle spherical. The higher Ca, the more elongated the particle's equilibrium shape. Moreover, if the value of the capillary number exceeds the critical capillary number, then the parent particle fragments into daughter particles via Plateau-Rayleigh instabilities. To draw an optical fiber, the temperature can be chosen between 1850 and 2150 °C. This 300 °C range corresponds to a change in viscosity of more than an order of magnitude. As a result, the capillary number, and hence the shape of the nanoparticles, can be modified as a function of the drawing conditions. The lower the drawing temperature, the more the particles elongate and fragment. It should be noted, however, that these elongation/fragmentation mechanisms are observed for particles larger than 50–100 nm. At the smallest particle sizes, there is no noticeable elongation. By increasing the drawing temperature, it is possible to exceed the binodal line (to leave the immiscibility gap), leading to nanoparticle melting [45]. Although the physical mechanisms have been identified, the prediction of particle elongation and fragmentation remains complex, as parameters such as particle viscosity and surface tension between the particles and the glass matrix are very difficult to determine.

4. Fiber lasers and amplifiers

4.1. Fabrication of nanoparticles-doped fiber lasers and amplifiers

This Section is focused on the study and development of nanoparticles and nanostructured doped glasses into optical fibers and their use in amplifiers and lasers. Here, unlike some of the other applications described in this Review, transparency is centrally important, as also is scalability and amenability with commercial fabrication methods, e.g., chemical vapor deposition.

As noted previously in section 3, there are two principal approaches to realizing nanoparticles or nanostructures in glasses and optical fibers, each having advantages and disadvantages reported in Table 1. For the purposes of this Section, the method by which the nanostructuring of the fiber core is achieved is not considered, unless central to the discussion. Instead, attention will be paid to the unique attributes of active nanostructuring and opportunities they afford to fiber amplifiers and lasers.

The first glass ceramic fiber amplifiers and lasers, based on neodymium [46], and then broadband emission using nickel as the dopant [26] were reported by scientists from Corning Incorporated.

The first report of using porous MCVD soot as a vehicle to include particles into the core of a subsequent preform and optical fiber is credited to *Yoo* et al., dated January 2003. They studied glass-ceramics in the (Co-doped) $ZnO–Al_2O_3–SiO_2$ (ZAS) system [47], which then were pulverized and formed into a slurry with fumed silica and subsequently solution doped into the preform soot. The ceramic phase is reported to have persisted following the MCVD and fiber draw process [47].

Given the commercial supremacy of telecoms at this time, it should not be surprising that attention soon turned to erbium-doped nanostructuring in fibers. In this regard, the work by Le Sauze and subsequent work by the Alcatel/Draka team is important [48]. It is instructive for the works that follow to discuss the purpose provided by La Sauze et al., in using this approach. As they state: "*Within the solution doping technique, certain limitations also exist concerning the achievable doping level and homogeneity due to the solubility and stability domains of rare-earth inorganic salts solutions and their tendency to self-associate into poorly defined chemical structures. These problems not only clearly impact on the fiber homogeneity but also result in the well-known concentration quenching phenomena that is among the most efficient dissipative processes responsible for EDF performance degradation when erbium concentration is increased* [48]."

Interestingly, the use of nanoparticles, whose sizes is approximately sub-wavelength, was a means to greater effective homogeneity since phase separation in sesquioxide-doped silica (Er_2O_3, Al_2O_3, etc.) can be more pronounced, leading to ion-ion clustering and quenching, and greater scattering. Indeed, shortly thereafter, in 2007, Podrazky et al., observed lower baseline attenuation values for (alumina) nanoparticle doped fibers, compared to conventionally prepared ones [49]. Put another way, while the two methods of "nanoparticle-doping" described in Section 3 can permit sub-wavelength nanostructures, using pre-synthesized NPs is arguably more controllable in terms of resultant NP sizes and concentrations, even if compositions may be more limited due to reactions with the host glass at the elevated processing temperature commonly employed in preform fabrication and fiber draw processes.

A subtle but historically important observation offered here is that in the original works by the Alcatel/Draka team [48,50] employed erbium-doping of the alumina nanoparticles to, as stated by Le Sauze et al., "… not only prevents erbium atoms from unwanted aggregation during the nanoparticle formation, that is crucial to avoid the deleterious erbium clustering phenomenon but will also allow the construction of the erbium environment thanks to the incorporation of specified co-dopants with a versatile flexibility." N. B. Core-shell (Al_2O_3 core/SiO_2 shell) NP analogs were first explored a few years later [51]. This is different from the subsequent work by Podrazky et al., in which undoped alumina nanoparticles were synthesized and doped into the MCVD soot [49]. The erbium dopant was solution doped per usual [4]. In this latter case, the erbium and alumina may not always be sufficiently proximate to be of spectroscopic benefit, even if the resultant fibers exhibited lower losses using alumina NPs, than when the alumina was solution doped.

A next important advancement was performed by *Kucera* et al. [52,53], who employed differently doped (Eu and Tb) nanoparticles to spatially separate and therefore control energy transfer between the Eu/Tb within the same silica glass preform. This work was the first to appreciate that NP doping could permit spectroscopic tailorability by sequestering each emitter in spatially separated nanoparticles and can be extended to high power fiber lasers [54]. Such dopant species partitioning, i.e., luminescence engineering, is generally not possible with conventional doping schemes, and followed on a previous concept of differently doped NPs in a polymer optical fiber for broadband amplification [55].

During this same period (2007–2010), advancements also were being made in NP-doped silica fibers based on phase-separated or

nucleation/growth core glass systems using CVD [56–60] or sol-gel [61, 62] as the means of fabrication. Though often treated as topically separate from inorganic nanoparticle doped optical fibers (e.g. Ref. [63], vs [64]), this period also witnessed foundational advancements in inorganic plasmonic- and quantum dot (QD)-doped optical fibers. More general reviews of NP-doped fibers of all these types can be found in Refs. [5,37,63–68], in particular, noble metal nanoparticles are discussed in Refs. [67,68].

Staying with considerations of scalability and practicality, e.g., low loss, plasmonic and QD-doped fibers fabricated based on MCVD preforms originated with the work of *Ju* et al., for plasmonic nanoparticles [69] and *Pang* et al. [70], for quantum dots, to the best of the Author's knowledge. For completeness, it is noteworthy that quantum dot-doped fibers date back to at least the late 1980s. In those early works, the fibers were fabricated either by rod-in-tube methods [71,72], CVD (e.g., VAD or thermal CVD) followed by solution doping or gas reactions [73], or by suspending quantum dot colloids in liquids or organics, which were then infused into the core of a capillary glass fiber [74]. In these early works, the focus on such fibers was towards enhanced nonlinearities.

Table 2 provides a chronological tabulation of papers on inorganic nanoparticle doped MCVD-derived silica optical fibers with a focus on those employed for lasers studies, in additional to foundational efforts. Apologies to those Authors not cited. Any oversight is due to the growing body of literature in the field of inorganic nanoparticle-doped fibers and the near impossibility of tracking all papers and advancements.

The sheer number of entries provided in Table 2, acknowledging the impossibility of its completeness, provides a sense of the interest and growing maturity of the field as well as the diversity of NP chemistries and range of active dopants. *N.B.*, Table 2 refers only to MCVD silica-based NP-doped optical fibers. This is because MCVD is a commercial process, employed through the silica optical fiber industry, and affords low loss silica fibers. This latter point is important for both practical applications and to best understand the role of the NPs on fiber performance, less obscured by extrinsic factors. NP-doped fibers have been made by other methods, including rod-in-tube [46,71,139] and melt-in-tube (i.e., molten core method) [140].

4.2. Applications

As suggested by Sub-Section 4.1 above, the applications of NP-doped fibers are as wide-ranging as the diversity of NP compositions/chemistries and dopants portrayed in Table 2. To this end, Table 3 provides a similar summary but by application.

In terms of applications of nanoparticle-doped fibers, as noted, it is unsurprising that much of the early work and a large portion of on-going efforts have focused on erbium doping. In the foundational works, the focus on erbium was due to the contemporary focus on erbium amplifiers for the then nascent telecommunications industry. Indeed, even the first work [47], which explored Co^{2+} doped glass-ceramic particles in MCVD silica noted interest in "silica glass based optical fibers for the active component applications such as an optical amplifier" in its Introduction. More explicit was the seminal contribution by *La Sauze* et al. [48], that directly bases its work on – as the title states – "Nanoparticle Doping Process: towards a better control of erbium incorporation in MCVD fibers for optical amplifiers." Erbium is also useful since it is extremely well characterized and the multiplicity of energy levels and transitions makes spectroscopic computations, e.g., Judd-Ofelt parameterization, and comparisons more straightforward.

Following the "dot.com" bubble bursting, focus began to shift towards non-telecom applications, including fibers lasers and non-erbium fiber amplifiers. The latter was driven over time by demands for higher power fiber-based systems employed for defense, sensing, and machining. As observed in Table 3, erbium remains a key dopant, though more specifically for eye-safer high power fiber amplifiers and lasers. EDFAs are generally considered mature technologies today, though recent work on Er:NP-doped EDFAs showing enhanced

Table 2
A chronology of MCVD-derived nanoparticle doped silica optical fibers.[a].

Doping Approach[b]	Precursor NP or Nucleating Agent	Active Dopant(s)	Publication Date[c]	Reference
SD	$ZnAl_2O_4$	Co^{2+}	2003 Jan 1	[47]
SD	Al_2O_3	Er^{3+}	2003 Jul 6	[48]
Sol gel	Au (plasmonic)		2006 Nov 1	[69]
SD	Si		2007 Jan 18	[75] [d]
SD	Au (plasmonic)		2007 May 14	[76]
Vaporization	InP		2007 Oct	[70]
SD	Al_2O_3	Er^{3+}	2007 Oct 21	[49]
SD + PS	CaO	Er^{3+}	2008 Jan 15	[56]
SD	PbSe (quantum dot)		2008 Feb 24	[77]
	Ag (plasmonic)		2008 Feb 24	[78]
SD + PS	CaO	Er^{3+}	2009 Feb 14	[57]
SD	Al_2O_3	Er^{3+}	2009 Feb 19	[50]
SD	LaF_3	Eu^{3+}/Tb^{3+}	2009 Aug 1	[52]
SD + PS	CaO	Er^{3+}	2009 Nov 1	[79]
SD	Al_2O_3	Er^{3+}	2010 Feb 17	[58]
SD	LaF_3	Eu^{3+}/Tb^{3+}	2010 Mar 21	[53]
SD	Y_2O_3/P_2O_5	Er^{3+}	2010 Oct 15	[59]
SD	YAG	Yb^{3+}	2010 Nov 25	[60]
NP solution spray	PbTe (quantum dot)		2011 Jan 31	[80]
SD	Al_2O_3	Er^{3+}	2011 Feb 10	[81]
SD + PS	MgO	Er^{3+}	2011 Aug	[27]
SD + PS	Al_2O_3, Y_2O_3, ZrO_2	Yb^{3+}	2011 Aug 1	[82]
SD	Al_2O_3	Er^{3+}	2012 Jan 30	[83]
SD	Al_2O_3	Er^{3+}	2012 Feb 15	[51]
SD + PS	ZrO_2	Er^{3+}	2012 Mar	[84]
SD + PS	Al_2O_3, Y_2O_3, ZrO_2	Yb^{3+}	2012 Feb 22	[85]
SD	CaF_2, SrF_2, BaF_2	Eu^{3+}	2012 Nov 1	[86]
SD + PS	MgO	Er^{3+}	2012 Nov 1	[87]
PS	ZrO_2	Er^{3+}	2013 Mar 30	[88]
SD	Al_2O_3	Er^{3+}	2014 Oct	[89]
SD + PS	MgO	Er^{3+}	2014 Oct 1	[90]
SD	YAG	Er^{3+}	2014 Dec 30	[91]
SD + PS	Y_2O_3	Tm^{3+}	2015 Feb 2	[92]
ALD	PbS (quantum dot)		2015 Apr 1	[93]
SD	$AlPO_4$	Yb^{3+}/Er^{3+}	2015 Jun 21	[94]
SD	Al_2O_3	Er^{3+}	2015 Jun 27	[95]
PS	YAG	undoped	2016 Mar 1	[43]
SD	Al_2O_3	Er^{3+}	2016 Mar 16	[96]
SD + PS	Y_2O_3	Yb^{3+}	2016 Oct 1	[66]
ALD	PbS (quantum dot)		2017 Feb 1	[97]
SD	LaF_3, Lu_2O_3	Ho^{3+}	2017 Mar 7	[98]
SD	LaF_3	Tm^{3+}	2017 May	[44]
SD	LaF_3	Tm^{3+}	2017 Jun 1	[99]
SD	Al_2O_3, LaF_3, Lu_2O_3	Er^{3+}, Ho^{3+}	2017 Jun 12	[52]
ALD	PbS (quantum dot)		2017 Jul 1	[100]
SD	LaF_3	Tm^{3+}	2018 May 17	[101]
SD	YAG	Er^{3+}	2018 May 21	[102]
SD	Al_2O_3	Tm^{3+}	2018 Sep 16	[103]
SD	Al_2O_3	Er^{3+}	2018 Sep 17	[104]
ALD	PbS (quantum dot)		2018 Sep 24	[105]
SD	Al_2O_3	Er^{3+}	2018 Nov 4	[106]
SD, SD + PS	LaF_3, MgO	Er^{3+}	2019 Jan 1	[107]
SD	Al_2O_3	Ho^{3+}	2019 Sept 11	[108]
ALD	PbS (quantum dot)		2019 Sep 15	[109]
SD + PS	MgO	Er^{3+}	2019 Nov 4	[30]
SD + PS	Alkaline earths	undoped	2020 Mar 3	[110]
PS	Y_2O_3	Tm^{3+}	2020 May 12	[111]
PS	CaO	undoped	2020 May	[112]
PS	ZrO_2	Tm^{3+}	2020 Jun 1	[113]
PS	CaO	undoped	2020 May	[114]
PS	ZrO_2	Tm^{3+}, Ho^{3+}	2021 Apr 18	[115]
PS	Y_2O_3	Tm^{3+}	2021 May 10	[116]
PS	MgO	undoped	2021 Aug 1	[117]
SD	Al_2O_3	Ho^{3+}, Er^{3+}, Tm^{3+}	2021 Aug 1	[118]
ALD	PbS (quantum dot)		2021 Aug 15	[119]
PS	Al_2O_3	Tm^{3+}	2021 Oct 3	[120]
SD	CaF_2, SrF_2, BaF_2	Yb^{3+}	2022 Mar 3	[121]
SD	YF_3	Yb^{3+}	2022 Mar 3	[122]
PS	Al_2O_3	Yb^{3+}	2022 Mar 4	[123]
PS	CaO	undoped	2022 Apr 1	[124]

(*continued on next page*)

Table 2 (*continued*)

Doping Approach[b]	Precursor NP or Nucleating Agent	Active Dopant(s)	Publication Date[c]	Reference
SD	LaF_3	undoped	2022 May 6	[40]
SD	Al_2O_3	Yb^{3+}, Tm^{3+}, Ho^{3+}	2022 Mar 14	[125]
SD	BaF_2	Yb^{3+}	2022 May 15	[126]
SD/PS	La_2O_3	undoped	2022 May 25	[45]
PS	CaO, MgO	undoped	2022 Jul 13	[127]
SD	CaF_2, SrF_2, BaF_2	Yb^{3+}, Eu^{3+}	2022 Oct 1	[41]
SD/PS	La_2O_3	undoped	2022 Nov 5	[128]
SD/Reaction	YAG, YPO_4	undoped	2023 Mar 14	[42]
SD	$YbPO_4$	Yb^{3+}	2023 Apr 1	[38]
PS	Al_2O_3, Y_2O_3	Yb^{3+}	2023 Apr 3	[129]
No details given but presumably same as in [128]			2023 Jun 1	[130]
PS	Y_2O_3	Yb^{3+}	2023 May 17	[131]
SD/Reaction	YAG, YPO_4	Yb^{3+}	2023 Aug 9	[132]
PS	Y_2O_3	Yb^{3+}	2023 Oct 1	[133]
PS/reaction	SiO,[e] YPO_4	undoped	2023 Dec 1	[134]
SD	Al_2O_3	Er^{3+}, Tm^{3+}	2024 Apr 1	[135]
SD	BaF_2	Er^{3+}	2024 Mar 24	[136]
SD	BaF_2	Dy^{3+}	Submitted	[137]

[a] Some papers are not included because they were not readily available. While not included in this Table, they are included in the References.

[b] Solution Doping (SD), Phase Separation (PS), Nucleation/Growth (NG), Modified Chemical Vapor Deposition (MCVD), Atomic Layer Deposition (ALD).

[c] Per Google Scholar.

[d] Seems to conflict with Pickrell [138] where MCVD SiO_2 doped with Si converted to SiO at the elevated processing temps to form holes/voids as a route to random hole optical fibers.

[e] SiO is generally a vapor, as in the case of it being used in Ref. [138] to, as noted above, form holes/voids as a route to random hole optical fibers. This seems to conflict with [134], who claim to have crystallized NPs of SiO.

properties may call this into question [136].

It is also useful to note that virtually all lanthanides have been studied in NP-doped silica fibers, including La (used to induce nucleation/phase separation), Pr [139] (though not MCVD or silica), Nd [46], Eu [53], Tb [53], Dy [137], Ho [98], Er [many; see Table 2], Tm [many; see Table 2], and Yb [many; see Table 2]. Quantum dots (e.g., Refs. [64, 68]) and select transition metals (e.g., Ni [26] and Co [47]) have also been explored.

The application of NP-doped fibers is predominantly focused on fiber amplifiers and lasers, hence this Section. However, there are a few emerging areas that are worthy of note. These include (i) nanoparticle/nanostructuring of the core to enhance scattering as applied to random fiber lasers [112,141], (ii) narrow linewidth fiber lasers [128,130], and (iii), the recent realization of anti-Stokes fluorescence cooling in silica fibers [121,122,126,129,131,133].

5. Distributed nanoparticles-doped fiber sensors

5.1. Optical backscatter reflectometry

Optical Fiber Sensors can be categorized based on their spatial capabilities, allowing them to perform point-wise measurements or extend along the fiber's length [142]. This classification includes three main categories: punctual, quasi-distributed, and distributed sensors [143]. Punctual sensors provide localized readings of the physical parameter of interest, while quasi-distributed sensors deliver parameter values across a distance and in relation to the fiber's position in discretized positions [144]. Distributed sensing relies on using an entire optical fiber span as a sensing element, interrogating the reflections occurring in every portion of the optical fiber due to Rayleigh, Brillouin, or Raman scattering [145]. Modern distributed sensing methods mainly rely on optical frequency-domain reflectometry (OFDR), which interrogate the fiber backreflection in the frequency domain using a Fourier transform of the reflected signals [146]. OFDRs use a scanning laser emitting at infrared

Table 3
Applications of NP-doped MCVD-derived silica fibers.

Reference	Application
[47]	Scientific inquiry
[48]	Erbium doped fiber amplifier (EDFA)
[69]	Plasmonics
[75]	EDFA
[76]	Plasmonics
[70]	Plasmonics
[49]	EDFA
[56]	EDFA
[50]	EDFA
[77]	Plasmonic amplifiers
[78]	Plasmonics/nonlinear optics
[57]	EDFA
[52]	Scientific inquiry/controlling energy transfer
[79]	EDFA
[58]	EDFA
[53]	Scientific inquiry/controlling energy transfer
[141]	Random fiber laser
[59]	EDFA
[60]	Up-conversion and high-power fiber lasers
[80]	Plasmonics/nonlinear optics
[81]	EDFA
[27]	Scientific inquiry/fiber lasers and amplifiers
[82]	Scientific inquiry/fiber lasers and amplifiers
[83]	Radiation resistant EDFA
[51]	EDFA/Scientific inquiry/fiber lasers and amplifiers
[84]	EDFA
[85]	High-power fiber lasers
[86]	Scientific inquiry/spectral engineering
[87]	Scientific inquiry/composition of NPs in silica
[88]	EDFA
[89]	EDFA
[90]	EDFA
[91]	EDFA
[92]	Fiber amplifiers/lasers (thulium @ 2 μm)
[93]	Plasmonics
[94]	Fiber amplifiers/lasers (ytterbium + erbium)
[95]	Fiber amplifiers/lasers (erbium)
[43]	Supercontinuum generation
[96]	Fiber amplifiers/lasers (erbium)
[66]	High-power fiber lasers/amplifiers
[97]	Plasmonics
[98]	Fiber amplifiers/lasers (holmium)
[44]	Scientific inquiry/fate of NPs during fiber processing
[99]	Fiber amplifiers/lasers (thulium @ 1.4 μm)
[54]	High-power fiber lasers/amplifiers
[100]	Plasmonics
[101]	Fiber amplifiers/lasers (thulium @ 1.4 μm)
[102]	Fiber amplifiers/lasers (erbium)
[103]	Fiber amplifiers/lasers (erbium)
[104]	EDFA
[105]	Plasmonic fiber sensors
[106]	Fiber amplifiers/lasers (erbium)
[107]	Scientific inquiry/fate of NPs during fiber processing
[108]	Fiber amplifiers/lasers (holmium)
[109]	Plasmonic fiber temperature sensors
[30]	Enhanced light scattering fibers
[110]	Scientific inquiry/fate of NPs during fiber processing
[111]	Fiber amplifiers/lasers (thulium @ 1.8 μm)
[112]	Random fiber laser
[113]	Fiber amplifiers/lasers (thulium)
[114]	Random fiber laser
[115]	Fiber amplifiers/lasers (thulium @ 2 μm)
[116]	Ultrafast mode-locked fiber lasers
[117]	Scientific inquiry/fate of NPs during fiber processing
[118]	Scientific inquiry/fate of NPs during fiber processing
[119]	Plasmonic fiber amplifiers
[120]	Scientific inquiry/fate of NPs during fiber processing
[121]	Laser cooling/radiation balanced fiber lasers and amplifiers
[122]	Laser cooling/radiation balanced fiber lasers and amplifiers
[123]	Fiber amplifiers/lasers (ytterbium)
[124]	Tunable distributed fiber sensors
[40]	Scientific inquiry/fate of NPs during fiber processing
[125]	Scientific inquiry/fate of NPs during fiber processing
[126]	Laser cooling/radiation balanced fiber lasers and amplifiers

(*continued on next page*)

Table 3 (*continued*)

Reference	Application
[45]	Scientific inquiry/fate of NPs during fiber processing
[127]	Scientific inquiry/fate of NPs during fiber processing
[41]	Scientific inquiry/fate of NPs during fiber processing
[128]	Narrow linewidth fiber laser
[42]	Scientific inquiry/fate of NPs during fiber processing/fiber lasers
[38]	Scientific inquiry/fate of NPs during fiber processing/fiber lasers
[129]	Laser cooling/radiation balanced fiber lasers and amplifiers
[130]	Narrow linewidth fiber laser
[131]	Laser cooling/radiation balanced fiber lasers and amplifiers
[132]	Distributed fiber sensors
[133]	Laser cooling/radiation balanced fiber lasers and amplifiers
[134]	Scientific inquiry/fate of NPs during fiber processing
[135]	Scientific inquiry/fate of NPs during fiber processing/fiber lasers
[136]	EDFAs
[137]	Visible fiber lasers

wavelengths into a single-mode fiber (SMF), and using demodulation process based on interferometry [147]; this allows achieving a spatial resolution $\Delta z = c/(2n_{eff}\Delta f)$ where c is the light speed, n_{eff} is the effective refractive index of the fiber, and Δf is the scanning bandwidth of the laser. OFDR systems achieve spatial resolution as low as 10 μm, which allows millimeter-scale sensing with high accuracy through spatial averaging.

Rayleigh scattering is an excellent source of information in OFDR signals. Each section of the fiber is characterized by random defects, that are consistent over time but have no correlation between multiple fiber sections [148,149]; the spectral response for each fiber section is a random signal, and the set of these random spectra collected at each Δz interval is the "signature" of the fiber. When the fiber is perturbed by physical quantities (temperature and strain), each spectral signature exhibits a wavelength shift that is proportional to these quantities (with coefficients of 10 p.m./°C and 1 p.m./με, respectively, at infrared wavelengths). Similar considerations can be performed when the fiber is perturbed, by chemical etching or tapering, in such a way that the effective refractive index is altered, and this effect can be exploited for refractive index sensing and biosensing. By analyzing the spectral shift of each fiber signature, one can measure the wavelength shift in each section of the fiber, which enables the distributed detection of physical parameters over long lengths with dense spatial resolution.

Telecom fibers are engineered to have Rayleigh scattering as low as possible, in order to obtain long-range transmission over hundreds of kilometers; this results in low values of Rayleigh scattering, around −120 dBm; despite this low power ratings, commercial optical backscatter reflectometer (OBR) units can still retrieve the fiber signatures with sufficient accuracy; these systems are commonly used in mechanical, geotechnical, and infrastructural monitoring [150]. In recent years, solutions to increment Rayleigh scattering in optical fibers have been considered, using a plurality of approaches that cater to different sensing needs. One method that has been reported, playing at the border between Rayleigh scattering enhancement and the inscription of reflective elements, is the use of long-range weak-reflective gratings having wide bandwidth. Methods have been reported using in-fiber nanogratings inscribed with a femtosecond laser [151], random optical gratings fabricated by interferometric setup [152], and continuous reflectors inscribed in the fiber core [153]. Another less sophisticated method relies on the exposure of a single-mode fiber to intense UV light [154].

While the previous methods are not very practical for sensing setups, because they rely on tagging specific fiber sections or inscribing localized sections of a fiber, methods based on the fabrication of fibers having large concentrations of nanoparticles or nano-defects in the fiber core are much more practical, since such fibers can be spooled, spliced to single-mode fibers in any arbitrary configuration, and form sensing networks operating in distributed sensing mode. This possibility has become increasingly important looking into biomedical applications: in this context, when working with compact and mini-invasive devices, it is not possible to operate with a single fiber arranged in a 2- or 3-dimensional configuration, but it is necessary to achieve a multi-fiber distributed sensing network in order to maintain a compact footprint. Thanks to the use of enhanced backscattering fibers (EBFs), having a high Rayleigh scattering thanks to the presence of a substantial concentration of scattering center in the fiber core, it is possible to create sensing networks that multiplex multiple EBFs while interrogating each of them as a distributed sensor with a single scan. This arrangement, labeled scattering-level multiplexing (SLMux), is sketched in Fig. 1(a). It is similar to a spatial-division multiplexing arrangement [155] spread through N channels using a 1xN splitter and using each SMF fiber as a delay line; at any interval of each EBF serving as sensing element, the obtained signature is the overlap of the EBF Rayleigh scattering, and up to (N-1) SMF fibers. Since the signatures are statistically independent on each other, and EBFs have substantial scattering increments (≫ 1000 times), the SLMux can interrogate each EBF independently, converting distributed sensing to a multi-fiber approach [156]. The two parameters characterizing an EBF are the scattering gain, which devices the increment of backscattered power over a SMF fiber, and the two-way fiber attenuation (that limits the sensing length per each channel).

Based on this approach, SLMux configurations enabled by the use of nanoparticle-doped fibers have been proposed; the main ones, sketched in Fig. 1(b–e) and listed in Table 4, employ EBF fibers to build multi-dimensional 2D or 3D sensing networks, or use the sensors for biological detection. One of the main applications of this sensing network is in thermal ablation of cancer, a mini-invasive methodology for deep-seated ablation of tumors that rely on a compact medical applicator that delivers a radiofrequency, microwave, or laser power that is dissipated into the tumors, heating up a well-confined region [157]. Temperature control is essential in this scenario, because thermal doses control the mortality rate of cancer cells; SLMux networks are the first ever approach to bring multidimensional temperature detection at the millimeter level of resolution and with rapid response of 1 s (limited by the OBR scanning frequency). This approach has been reported in 2D configurations, using 4–6 fibers having sensitivity 9.4–11.9 p.m./°C. The first work was reported in 2019 by Beisenova et al. [156] for radiofrequency (RF) ablation, pioneering this sensing concept; the 2D sensing network is achieved by detecting distributed data (2.5 mm resolution) in each EBF fiber, and vertically spacing multiple fibers few millimeters apart, achieving temperature sensing over a 2.5 × 5.0 mm pixel-size grid. This approach was then applied to resolve thermal distributions in several cancer ablation scenarios, including RF ablation mediated by nanoparticles [158], RF ablation neighboring blood vessels [159], and laser ablation of parenchymal tissue mediated by nanoparticles [160]. 3D temperature sensing was also achieved expanding the SLMux to 12 fibers, the maximum numbers reported so far, achieving a density of 144 sensors in a 16 x 16 × 25 mm region (22.5 sensors/cm^3), which is the highest resolution observed for *in situ* temperature detection using sensors [161].

Another biomedical application that is emerging for its importance in clinical and diagnostic practice is the possibility of performing a real-time shape sensing of a surgical device, relying on multi-dimensional strain measurements [170]. SLMux configurations have been reported for shape sensing of rigid device, by installing up to 4 fibers along the needle. Each small bending of the needle transfers a different amount of strain to each section of the fiber; since the needle is rigid, a shape reconstruction algorithm can be implemented by estimating the local strain in each direction, and therefore estimating the 3-dimensional bending angle [163]. This approach was established and validated for epidural devices, used in clinical practice for administering epidural anesthesia, [164]; the 3D shape sensing observed in real time with error ± 1%, can be used as a guidance system for manual insertion of the epidural device through the multiple subcutaneous layers reaching the epidural space. The approach reported in Ref. [162] disambiguates temperature effects from strain, estimating the depth of penetration and compensating for the different temperature of the body and its external

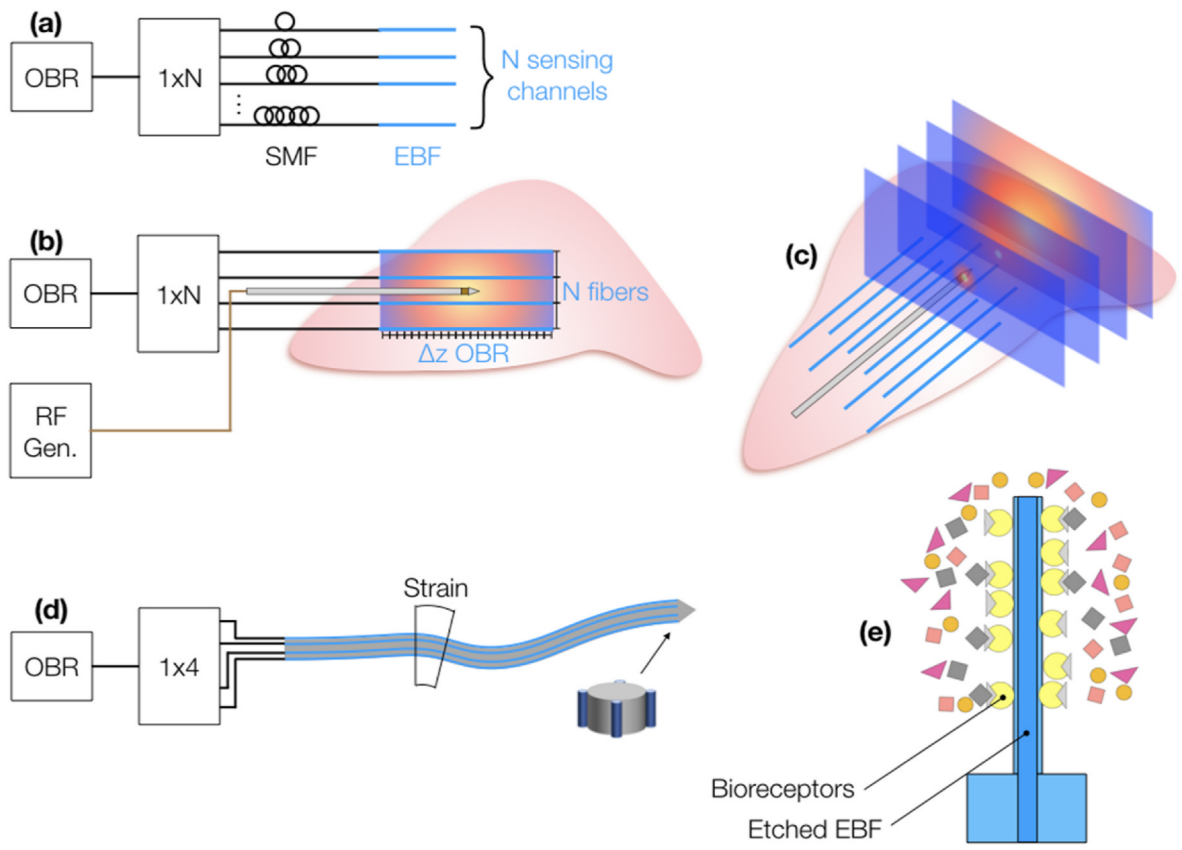

Fig. 1. Schematic of SLMux approach and sensing networks derived from it for biomedical applications, enabled by nanoparticle-doped EBF fibers. (a) Schematic of a generic N-channel SLMux distributed sensing setup. (b) Sketch of RF ablation of cancer tissues, with 2D sensing network; (c) 3D sensing networks in RF ablation. (d) Distributed shape sensing of medical devices. (e) Schematic of a reflector-less biosensor functionalized with bio-receptors for protein sensing.

Table 4
Overview of the most significant distributed sensing applications of high-scattering, nanoparticle-doped fibers.

Application	# Sensing fibers	Scattering gain	Attenuation	Detected parameter	Sensitivity	Reference
Radiofrequency ablation of cancer	4	36.5 dB	25.5 dB/m	Temperature	11.9 p.m./°C	[156]
Radiofrequency ablation of cancer	12	15–40 dB		Temperature	10.25 p.m./°C	[161]
Radiofrequency ablation, assisted by nanoparticles	6	~40 dB		Temperature	9.4 p.m./°C	[158]
Radiofrequency ablation of cancer	6			Temperature	~10 p.m./°C	[159]
Laser ablation of cancer, assisted by nanoparticles	6	>30 dB		Temperature	10.4 p.m./°C	[160]
Teperature-compensated 3D shape	4	45 dB		Strain + temperature	8.04 p.m./°C; 1.04 p.m./με	[162]
Epidural needle 3D shape sensing	4	45 dB	33 dB/m	Strain	1 p.m./με	[163]
Epidural needle 3D shape sensing	4	35–40 dB		Strain	1 p.m./με	[164]
Dental bite force monitoring	8	~40 dB	~40 dB/m	Strain/pressure	2.376 p.m./kPa	[165]
Thrombotic biomarker aptasensing	1	50 dB	61.5 dB/m	Thrombin concentration	5.5 p.m./(μg/mL)	[166]
Cancer biomarker biosensor	3	43.7 dB		CD44 concentration (RI)	1.8 p.m./$\log_{10}$[pM] (−1.325 nm/RIU)	[167]
Refractive index sensing	1	45.3 dB	32.8–67.6 dB/m	Refractive index	3.7–45.9 nm/RIU	[168]
X-ray irradiation detection	1			Radiation dose	0.019 p.m./Gy	[169]

ambient. The more recent work of Katrenova et al. [165] expands the strain sensing concept to dental devices, by designing a bite force estimation system with 8 fibers that detects and localizes the force applied from a tooth onto a dental bite.

Biological applications have also been reported for EBF fibers. In this context, the increment of backscattering is an essential resource for the fabrication of "reflector-less" sensors, which operate as reflective probes interrogating the backscattering signal without the inscription of a reflective device (such as a grating or an interferometer). The refractive index (RI) sensitivity can be achieved by exposing the fundamental mode to the surrounding environment, either by etching the fiber cladding, or tapering the fiber to a narrower thickness. The etching process is slower but can be implemented in volume for a multitude of fibers [171], while the tapering process can be rapidly performed with a CO_2 laser splicer in about 1 min time [172]. Once the RI sensitivity is achieved, to levels around or higher than 1 nm/RIU (refractive index units), the fiber can be biofunctionalized by immobilizing a bioreceptor (such as an antibody or an aptamer) and perform a detection of a

biomarker even at low concentrations [173]. The first work describing a reflector-less biosensor was reported by Sypabekova et al. [166], using hydrofluoric wet-etching to remove the cladding of a nanoparticle-doped fiber. The increment in scattering is essential, since it compensates for the propagation losses (over 20 dB) due to evanescent light at the sensing point. With this arrangement, using an OBR interrogator, a distributed detection was achieved, with sensitivity up to 1.2 nm/RIU; using an aptamer as a bioreceptor immobilized with a gold coating, thrombin biomarker was detected with limit around 1 μg/mL. By improving wet-etching, Aitkulov et al. subsequently reported an increment in sensitivity up to 45.9 nm/RIU using the same distributed sensing hardware [168]. More recently, Shaimerdenova et al. reported a reflector-less biosensor based on a shallow fiber taper fabricated with 28 μm waist diameter [167]. This sensing device reported average sensitivity of 1.05 nm/RIU and was functionalized for the detection of CD44 cancer biomarker with detection limit of 16.4 pM. Following a similar pattern, the nanoparticle-doped EBF fibers have been also employed in the detection of X-ray doses, interrogating the change in effective refractive index occurring in the fibers when exposed to ionizing radiation; the work reported by Olivero et al. [169] shows a sensitivity of 0.019 p.m./Gy in various irradiation conditions.

5.2. *Transmission-Reflection Analysis and artificial intelligence algorithms*

In the last few years, the popularization of machine learning methods resulted in new pathways in scenarios for sensors applications, where the artificial intelligence (AI) algorithms can enhance the sensor performance [174], provide new insights and measurements from feature extraction [175] as well as provide the possibility of sensor fusion in heterogeneous sensing networks [176]. Such popularization in AI algorithm favors the development of distributed optical fiber sensors as well, where there are numerous reports on the use of AI algorithm in distributed optical fiber sensors as summarized in Ref. [177]. In distributed optical fiber sensors applications, the use of AI-based approaches can address in key challenge in the effective deployment of such sensors by providing an efficient processing and interpretation of the large volumes of data generated by these systems [178]. As the monitoring capabilities of these sensors continue to expand, the need for intelligent algorithms to extract meaningful insights from the data has become increasingly crucial [179]. In addition, AI algorithms aid on the decision-making process with the use of specific classifiers for different applications and conditions [180].

Despite the many advantages of distributed optical fiber sensing due to their spatially resolved data and high accuracy/detection limits, there are some limitations in such an approach, which can partially affect some sensors applications. In this context, one of the main limitations of distributed optical fiber sensors is their general high cost, since such approaches have acquisition system with bulk and costly components such as modulated light sources and, in some cases, microwave photonic circuits [181]. It is important to mention that such high cost can limit the use of distributed optical fiber sensors in healthcare applications, especially in remote healthcare, where the cost-effective requirements are of crucial importance [182]. Furthermore, the portability of the system is directly affected by the bulk components used in conventional distributed optical fiber sensors approaches, where such components mainly affect the possibility of using such approach in wearable devices [183].

One of the distributed optical fiber sensing approaches to tackle conventional distributed sensors (mainly based on OFDR in different configurations), the Transmission-Reflection Analysis (TRA) offers a cost-effective method for distributed sensing of mechanical disturbances along the optical fiber cable [184]. This method relies on directly measuring the transmitted and backscattered optical powers of an unmodulated continuous wave light source [185]. Such features enable the use of low-cost light sources (or even light emitting diodes) for the sensor development, providing not only a lower cost for the sensor system, but also higher portability of the devices [186]. In addition, the use of only photodetectors on the signal acquisition generally helps with further cost reduction and portability of the TRA-based distributed optical fiber sensor system.

In contrast to the OFDR method, which achieves high spatial resolution (~mm) [187], the TRA method exhibits lower spatial resolution (~m) when used with standard silica fibers [188]. This limitation stems from the weak Rayleigh backscattering signal of standard silica optical fibers [154]. One previously proposed method to enhance the reflected power and consequently improve spatial resolution, multiple fiber Bragg gratings (FBGs) can be inscribed into the fiber core [189]. However, implementing such FBGs without protective coatings may compromise the sensor's robustness. Moreover, the Bragg grating inscription in different materials involves the need of specialized equipment such as UV laser, phase mask, optical lenses, and kinematic mirrors, which can harm the TRA precedents of simple solution and low-cost setup [189]. As another crucial issue in TRA approach, the first developments in the technique indicated the possibility of measuring only one mechanical disturbance at a time for the TRA-based systems [185]. Thus, the conventional signal analysis of TRA approach uses a set of transmitted optical power as a function of the backscattered optical power on the fiber, where each transmission and reflection pair Fig. 2 is related to a position of the mechanical disturbance along the optical fiber cable [190]. For this reason, it is possible to verify that initially proposed TRA approach presents two major limitations: (i) poor spatial resolution due to small Rayleigh backscattering of standard silica optical fibers; (ii) only one simultaneous region for mechanical disturbance detection due to the limitations on the signal processing.

To mitigate the limitations conventionally observed in the TRA approach, the use of high scattering medium in optical fibers can enhance the spatial resolution of the TRA-based sensor systems, where the spatial resolution in this case can be as small as a few centimeters [190]. To that extent, the development of nanoparticle (NP)-doped optical fibers leads to enhanced Rayleigh backscattering which resulted in an important breakthrough on the development of cost-effective distributed optical fiber sensors. In this context, the comparison between the standard single mode fibers and a NP-doped optical fiber with enhanced backscattering is presented in Ref. [190]. The use of NP-doped fibers indicated an enhancement in the spatial resolution of 3 orders of magnitude, where the spatial resolution of around 1 m using standard

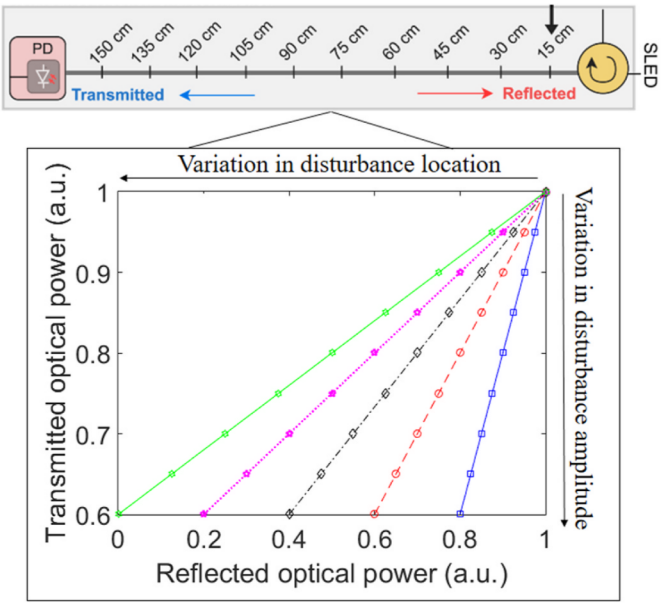

Fig. 2. Schematic representation of the operation principle of TRA approach.

single mode fiber was increased to around 6 mm using Magnesium and Erbium co-doped fiber [190]. However, it is important to mention that numerous compositions of the nanoparticles can be proposed and fabricated [37]. To that extent, the analysis of TRA responses using different optical fibers compositions was developed in Ref. [191]. In this case, different NP-doped optical fibers are subjected to sequential mechanical disturbances (with macro bending in a limited region of the NP-doped fiber) using the same experimental setup for the comparison of the spatial resolution and signal-to-noise ratio as well as the accuracy and attenuation. It is possible to observe that the particles size and composition directly affects the sensor response using the TRA method, since the NP sizes of around 100 nm resulted in larger attenuation, but with also larger reflectance. Table 5 presents a comparison between the NP-doped fibers (with 3 different compositions) with the standard silica single mode fiber as a function of performance parameters analyzed in TRA approach, namely accuracy, spatial resolution, attenuation and reflectance. It is worth to mention that such resulted were obtained from previous works of NP-doped optical fiber characterizations [20,190,191] in which the superior performance in terms of spatial resolution is verified for all NP-doped fibers when compared with the standard single mode fiber. Therefore, the use of NP-doped optical fiber addresses the first aforementioned major limitation of the TRA method, i.e., the poor spatial resolution due to small Rayleigh backscattering.

As the second mentioned limitation of TRA approach, the signal processing method using both transmission and reflection optical powers in a linear regression provides limitations related to the superposition of different simultaneous mechanical disturbances along the optical fiber cable [190]. In this context, the nonlinear modeling of the relation between mechanical disturbance amplitude and location as a function of transmitted and backscattered optical signal can provide insights on the multiple disturbances detection and on the overall system performance related to simultaneous assessment of disturbances amplitude and location [192]. For this reason, the use of machine learning methods, especially neural networks can enhance the sensor performance in signal processing, since it uses nonlinear models for data analysis. To that extent, the use of a feed-forward neural network (FFNN) for the TRA approach was proposed in Ref. [192], where a FFNN with two hidden layers (with 600 and 300 nodes) was developed to classify the mechanical disturbance location at six predefined regions. The goal is to classify the position of the mechanical disturbance with simultaneous disturbances and with different disturbances amplitudes. The proposed method using the TRA in conjunction with a FFNN resulted in the possibility of detecting up to three simultaneous mechanical disturbances along a single NP-doped optical fiber with an accuracy of 99.43% [192]. This result opens new pathways for the cost-effective distributed optical fiber sensing, where the second major limitation of TRA approach (i.e., single disturbance analysis at a time) is partially mitigated, where the use of the sensor system for up to 3 simultaneous disturbances opens a variety of applications scenarios, especially in healthcare.

Following the developments in the TRA method that mitigated both major limitations of this cost-effective distributed optical fiber sensing technique, wearable and non-wearable healthcare applications were proposed. Considering the wearable applications, a current approach for wearable sensor system is the use of smart textiles, where the fabrics and clothing accessories have embedded sensors [193]. The advantageous features and benefits of optical fiber sensors make them an useful tool for smart textiles development, or the so-called photonic textiles, where the optical fiber sensors are integrated in the textiles and clothing [194,195]. Following this background, a smart textile using NP-doped fibers was proposed in Ref. [196], where the TRA approach was employed for the disturbance location and amplitude assessment in the proposed smart textile. In this case, the proposed smart garment is used on the balance assessment during walking activities, which is an important analysis in biomechanics [197]. The NP-doped optical fiber is integrated into the smart garment, whereas the electronics unit (with the light sources, couplers and photodetectors) are positioned in a pocket on the proposed smart device (see Fig. 3). The validation tests included different mechanical disturbances applied at different regions of the proposed NP-doped fiber sensor system, where it is possible to verify a feasibility of the device, since the disturbance location estimation presented relative errors as low as 3.7% [196]. In addition, disturbance tests performed at standing and walking conditions indicated the suitability of the proposed device in detecting the disturbances under different movement conditions.

An important application in healthcare, especially in the field of digital health, is the remote and real-time monitoring of patients [198]. In this context, the development of smart homes and general environments with remote connectivity tackles many of the demands in digital health [199]. In view of such an important application and considering the major breakthrough of cost-effective distributed optical fiber sensors using NP-doped optical fiber, a heterogeneous smart home using optical fiber sensors was proposed in Ref. [200]. The proposed Opto-Electronic Smart Home uses the NP-doped optical fibers in TRA approach in conjunction with the AI algorithms for the localization of the patient in the home [200]. It is also worth noting that the smart home also includes an FBG-embedded carpet and a smart textile for movement analysis. However, the use of NP-doped fibers are restricted to the patient localization in the smart home, where the NP-doped optical fibers were integrated in the floor distributed along the proposed home. If the patient (or patients, since the analysis of 3 simultaneous users was performed in Ref. [192]) steps on a predefined region in a specific room steps on a predefined region in a specific room of the house, there is the classification (via FFNN approach) of the position of the patient. These data not only can be storage, but can also be sent to the health professional. A schematic representation of the proposed device is presented in Fig. 3, where it is possible to observe the position of the interaction regions (and NP-doped optical fibers) inside the smart home. Considering the application in smart textiles, the fiber small dimensions enable its integration into the textile using different approaches, which include not only the direct integration in the textile by stitching, but also the use of patches with embedded optical fiber that can be integrated to the clothing by a Velcro connection. This latter approach makes it easier for the fiber removal during clothing washing.

Table 5
Comparison between standard single mode fiber and NP-doped optical fibers for the TRA approach.

Fiber	NP Composition	Attenuation	NP size	Spatial resolution
SMF	–	0.0004 dB/m	–	0.25 m
I29	1 M $MgCl_2$(ring), 1 M $AlCl_3$, 0.01 M $ErCl_3$(core)	2.21 dB/m	40 nm	6.7 mm
G18-01	0.1 M $CaCl_2$, 0.01 M $ErCl_3$	68.53 dB/m	100 nm	30 mm
G21-01	0.1 M $SrCl_2$, 0.01 M $ErCl_3$	57.08 dB/m	100 nm	10 mm

6. Conclusion and prospects

Despite initial concerns about the introduction of nanoparticles into optical fibers due to light scattering, this review article highlights the wide-ranging potential of this approach. Successes include possible modifications of luminescence properties for lasers and amplifiers and, more unexpectedly, the use of light scattering to create new optical fiber architectures. Open questions and prospects are now discussed.

7. Light scattering

As far as the impact of nanoparticle characteristics on light scattering is concerned, the trends described in section 2 are deduced from results

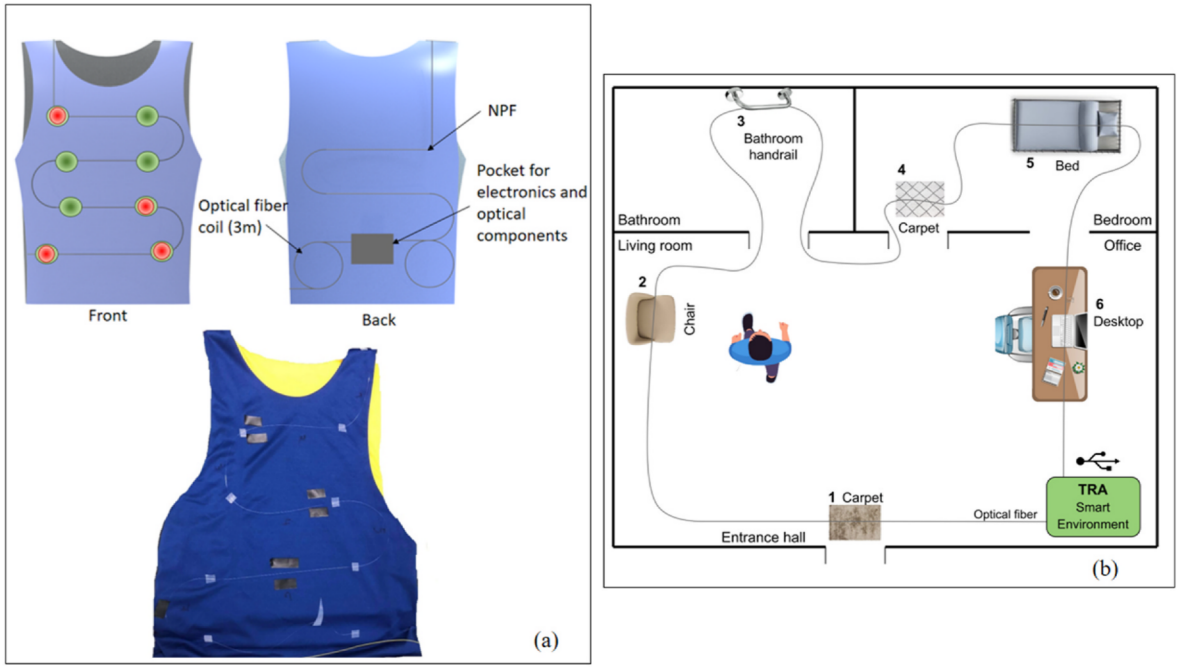

Fig. 3. NP-doped optical fibers in TRA overview for wearable and non-wearable healthcare applications. (a) Development of TRA-based distributed sensor systems for wearable monitoring in smart clothing. (b) Application of TRA distributed system using the NP-doped optical fibers for remote smart home monitoring.

observed mainly in bulk material. We now need to improve our understanding of nanoparticle-induced scattering in optical fibers, by considering the effect of size distribution, nanoparticles shape and the variation of their refractive index with their sizes. Another approach to control the light propagation in such a scattering medium could be based on shaping the wavefront [201].

8. Nanoparticle formation

As far as manufacturing processes are concerned, a better understanding of the reactivity of nanoparticles with the glass matrix will enable us to identify "stable" compositions or anticipate their transformation into another type of nanoparticle. Such studies will require a deeper understanding of thermodynamic mechanisms, particularly for nanoparticle formation via phase separation or nucleation/growth mechanisms. As for the mechanisms inducing particle elongation and fragmentation, it is essential to improve our ability to determine parameters such as particle viscosity or surface tension between particles and the glassy matrix.

9. Fabrication process

New manufacturing methods are currently being developed. For example, it is proposed to modify the characteristics of nanoparticles in optical fibers by irradiating them with a femtosecond laser [202]. The use of this laser enables only the core to be heated, thanks to a multi-photon interaction that enables μm resolution to be achieved. By controlling the laser parameters (e.g. repetition rate), it is possible to heat to different temperatures, enabling the nanoparticles to grow or dissolve. Using a reel-to-reel set-up, this approach would enable the characteristics of the nanoparticles to be varied along the fiber, at the μm scale. Finally, manufacturing processes based on additive synthesis could also open up new prospects for the preparation of optical fibers containing nanoparticles.

10. Laser

As noted, fiber laser and amplifier require minimum scattering (and loss) to achieve high efficiency and low thresholds, which tends to conflict with the concept of heterogeneous fibers. However, as witnessed by the number of works enumerated in this Section, maintaining low loss and scattering is possible when processing of the nanoparticle/nanostructured fibers is carefully controlled. There remains a lingering question: Are NP-doped fiber better than conventionally doped fibers when it comes to amplifiers and lasers?

Indeed, there is some evidence for the case of enhanced performance, but it cannot be said in general. This is because most of the published works do not offer a true comparison with the same core compositions, doping levels, etc. The answer also depends critically on what precisely is the molecular structure about the active dopant and how that local structure influences its spectroscopy. The answer also depends, of course, on the chemistry of the nanostructure, how it originates (suspension doping vs phase separation), whether it is crystalline or amorphous, the solubility of the dopant in the nanostructured region in the silica glass, the preform and fiber draw conditions, to name just a few. This is one reason there have been a fair number of recent papers investigating the "life of a nanoparticle" in silica as it is processed [38,40–42,44,45,107,110,117,118,120,125,127,134,135]. This is what makes this a very complex and multi-faceted problem to solve and why a generalized "yes" or "no" response is impossible.

That said, there are indications in select systems of enhanced spectroscopic properties of value to fiber amplifiers and lasers, including longer radiative lifetimes when the active species (e.g., Tm [99] and Dy [137]) is sequestered in a low phonon energy nanostructure. The recent work by Campbell suggests that Er:NP fibers can exhibit equal efficiency but at higher doping concentrations (or slightly higher efficiency at equal doping levels) than conventionally doped EDFAs [136]. Known also is the ability to isolate different emitters into different NPs, co-doped into the same silica core to control or mitigate energy transfer [54]. For intrinsically efficient emitters with few excited states, such as Yb, there does not seem to necessarily be a direct advantage, though secondary advantages (such as higher local doping or controlling energy transfer or upconversion) may be beneficial overall.

11. Distributed sensing

Looking at the perspectives on distributed sensing, the control of scattering properties of single-mode optical fibers is a key asset in the achievement of large multiplexing factors, moving the OBR technology from a single-channel layout to multi-dimensional and multi-parametric sensors; the coexistence of physical parameters (such as temperature and strain), biological analytes, and the possibility to enable chemical/radiation parameters can enable a wide range of detected parameters, as reported for other fiber-optic technologies [64], but maintaining a high density of sensing points, in 2D/3D geometries that are compatible with mini-invasive medical devices. From a system point of view, the network of fiber extenders needed to spatially multiplex the EBF can be integrated into a single device, that can be directly plugged in to commercial OBR/OFDR hardware. In terms of the design of the fibers, the trade-off between scattering gain and attenuation plays a significant role in determining the maximum reach of the sensing fibers, particularly when exposed to etching or tapering extra losses; a low-loss nanoparticle-doped fiber might extend the sensing length about or over the meter, and this might enable multi-fiber distributed sensors for applications that involve colonoscopy-based diagnostic [203], or cardiac applicators [204].

The use of NP-doped fibers in TRA approach and their combination with machine learning methods resulted in an important breakthrough in distributed optical fiber sensing, where such approaches can be used in cost-effective applications in which the cost of the sensor system is a major requirement. In this context, the proposed approach using cost-effective distributed optical fiber sensing led to healthcare applications in wearable and non-wearable systems. Following these developments, future perspectives for the use of NP-doped fibers in TRA approach include additional applications in shape reconstruction of structures for different applications as well as the instrumentation of flexible wearable robots. In addition, future perspectives include the improvements on the TRA technique itself, where NP-doped fibers with different compositions can be used to provide different Rayleigh Backscattering signatures as well as the use of wavelength filters to provide an additional possibility of enhancing the multiplexing capabilities of the TRA-based NP doped optical fiber sensor system.

CRediT authorship contribution statement

Wilfried Blanc: Writing – review & editing, Writing – original draft. **Daniele Tosi:** Writing – review & editing, Writing – original draft. **Arnaldo Leal-Junior:** Writing – review & editing, Writing – original draft. **Maurizio Ferrari:** Writing – review & editing. **John Ballato:** Writing – review & editing, Writing – original draft.

Declaration of competing interest

The authors declare that they have no known competing financial interests or personal relationships that could have appeared to influence the work reported in this paper.

Acknowledgments

W. Blanc, J. Ballato and M. Ferrari acknowledge membership of technical committees of photonic glasses and optical fibers (TC20) of International Commission on Glass (ICG). D. Tosi acknowledges the support of Nazarbayev University, under grant M2O-DISK (code: 20122022FD4134)

Data availability

No data was used for the research described in the article.

References

[1] K.C. Kao, G.A. Hockham, Dielectric-fibre surface waveguides for optical frequencies, Proceed. Institut. Electr. Eng. 113 (7) (1966 Jul 1) 1151–1158 (IET Digital Library).
[2] R.J. Mears, L. Reekie, I.M. Jauncey, D.N. Payne, Low-noise erbium-doped fibre amplifier operating at 1.54 μm, Electron. Lett. 19 (23) (1987) 1026–1028.
[3] Y.E. Jeong, J.K. Sahu, D.N. Payne, J. Nilsson, Ytterbium-doped large-core fiber laser with 1.36 kW continuous-wave output power, Opt Express 12 (25) (2004 Dec 13) 6088–6092.
[4] J.E. Townsend, S.B. Poole, D. Payne, Solution-doping technique for fabrication of rare-earth-doped optical fibres, Electron. Lett. 7 (23) (1987) 329–331.
[5] W. Blanc, J. Ballato, M. Ferrari, Glass for photonics, Eur. Phys. J. Plus 138 (2023 Sep 27) 858.
[6] https://www.youtube.com/watch?v=g9BL7vUjUfU.
[7] Y. Tamura, H. Sakuma, K. Morita, M. Suzuki, Y. Yamamoto, K. Shimada, Y. Honma, K. Sohma, T. Fujii, T. Hasegawa, The first 0.14-dB/km loss optical fiber and its impact on submarine transmission, J. Lightwave Technol. 36 (1) (2018 Jan 1) 44–49.
[8] F. Auzel, D. Pecile, D. Morin, Rare earth doped vitroceramics: new, efficient, blue and green emitting materials for infrared up-conversion, J. Electrochem. Soc. 122 (1) (1975 Nov 1) 101.
[9] J. Ballato, P. Dragic, Glass: the carrier of light-a brief history of optical fiber, Int. J. Appl. Glass Sci. 7 (4) (2016 Dec) 413–422.
[10] H. Zheng, Y. Hu, J.D. Mackenzie, Bi4Ca3Sr3Cu4Oy ceramic fibers from crystallization of glasses, Appl. Phys. Lett. 55 (12) (1989 Sep 18) 1255–1257.
[11] H. Zheng, Y. Hu, J.D. Mackenzie, Continuous drawing of Bi-Ca-Sr-Cu-O glass fibers from a preform, Appl. Phys. Lett. 58 (15) (1991 Apr 15) 1679–1681.
[12] Y. Wang, J. Ohwaki, New transparent vitroceramics codoped with Er3+ and Yb3+ for efficient frequency upconversion, Appl. Phys. Lett. 63 (24) (1993 Dec 13) 3268–3270.
[13] P.A. Tick, Are low-loss glass–ceramic optical waveguides possible? Opt Lett. 23 (24) (1998 Dec 15) 1904–1905.
[14] C.F. Bohren, D.R. Huffman, Absorption and Scattering of Light by Small Particles, John Wiley & Sons, 2008 Sep 26.
[15] T. Dunch, S.D. Jackson, Rayleigh scattering with material dispersion for low volume fraction transparent glass ceramics, Opt. Mater. Express 12 (7) (2022 Jul 1) 2595–2608.
[16] R. Apetz, M.P. Van Bruggen, Transparent alumina: a light-scattering model, J. Am. Ceram. Soc. 86 (3) (2003 Mar) 480–486.
[17] S. Asano, G. Yamamoto, Light scattering by a spheroidal particle, Appl. Opt. 14 (1) (1975 Jan 1) 29–49.
[18] A. Ishiniaru, Y. Kuga, Attenuation constant of a coherent field in a dense distribution of particles, JOSA 72 (10) (1982 Oct 1) 1317–1320.
[19] A.K. Ghatak, K. Thyagarajan, An Introduction to Fiber Optics, Cambridge university press, 1998 Jun 28.
[20] M. Silveira, C. Díaz, L. Avellar, W. Blanc, C. Marques, A. Leal-Junior, Characterization of optical fibers doped with nanoparticles for distributed displacement sensing, Opt Express 32 (6) (2024 Mar 11) 9610–9624.
[21] E. Brinkmeyer, Analysis of the backscattering method for single-mode optical fibers, JOSA 70 (8) (1980 Aug 1) 1010–1012.
[22] E.G. Neumann, Analysis of the backscattering method for testing optical fiber cables, Arch. Elektr. Uebertragung 34 (1980 Apr) 157–160.
[23] M. Nakazawa, Rayleigh backscattering theory for single-mode optical fibers, JOSA 73 (9) (1983 Sep 1) 1175–1180.
[24] T. Lee, M. Beresna, A. Masoudi, G. Brambilla, Enhanced-backscattering and enhanced-backreflection fibers for distributed optical fiber sensors, J. Lightwave Technol. 41 (13) (2023 Jun 7) 4051–4064.
[25] G. Liu, B. Jacquier (Eds.), Spectroscopic Properties of Rare Earths in Optical Materials, Springer Science & Business Media, 2006 Jan 29.
[26] B.N. Samson, L.R. Pinckney, J. Wang, G.H. Beall, N.F. Borrelli, Nickel-doped nanocrystalline glass-ceramic fiber, Opt Lett. 27 (15) (2002 Aug 1) 1309–1311.
[27] W. Blanc, V. Mauroy, L. Nguyen, B.N. Shivakiran Bhaktha, P. Sebbah, B.P. Pal, B. Dussardier, Fabrication of rare earth-doped transparent glass ceramic optical fibers by modified chemical vapor deposition, J. Am. Ceram. Soc. 94 (8) (2011 Aug) 2315–2318.
[28] G.A. Kumar, C.W. Chen, J. Ballato, R.E. Riman, Optical characterization of infrared emitting rare-earth-doped fluoride nanocrystals and their transparent nanocomposites, Chem. Mater. 19 (6) (2007 Mar 20) 1523–1528.
[29] D. Pugliese, N.G. Boetti, J. Lousteau, E. Ceci-Ginistrelli, E. Bertone, F. Geobaldo, D. Milanese, Concentration quenching in an Er-doped phosphate glass for compact optical lasers and amplifiers, J. Alloys Compd. 657 (2016 Feb 5) 678–683.
[30] W. Blanc, I. Martin, H. Francois-Saint-Cyr, X. Bidault, S. Chaussedent, C. Hombourger, S. Lacomme, P. Le Coustumer, D.R. Neuville, D.J. Larson, T. J. Prosa, Compositional changes at the early stages of nanoparticles growth in glasses, J. Phys. Chem. C 123 (47) (2019 Nov 4) 29008–29014.
[31] X.Y. Chen, H.Z. Zhuang, G.K. Liu, S. Li, R.S. Niedbala, Confinement on energy transfer between luminescent centers in nanocrystals, J. Appl. Phys. 94 (9) (2003 Nov 1) 5559–5565.
[32] G.K. Liu, H.Z. Zhuang, X.Y. Chen, Restricted phonon relaxation and anomalous thermalization of rare earth ions in nanocrystals, Nano Lett. 2 (5) (2002 May 8) 535–539.
[33] R.S. Meltzer, S.P. Feofilov, B. Tissue, H.B. Yuan, Dependence of fluorescence lifetimes of Y2O3:Eu3+ nanoparticles on the surrounding medium, Phys. Rev. B. 60 (20) (1999 Nov 15) R14012.

[34] R.S. Meltzer, W.M. Yen, H. Zheng, S.P. Feofilov, M.J. Dejneka, Relaxation between closely spaced electronic levels of rare-earth ions doped in nanocrystals embedded in glass, Phys. Rev. B 66 (22) (2002 Dec 13) 224202.

[35] E. Ma, Z. Hu, Y. Wang, F. Bao, Influence of structural evolution on fluorescence properties of transparent glass ceramics containing LaF3 nanocrystals, J. Lumin. 118 (2) (2006 Jun 1) 131–138.

[36] D.R. Neuville, L. Cormier, D. Caurant, L. Montagne, From glass to crystal: nucleation, growth and phase separation: from research to applications. Les Ulis, EDP Sciences, 2017.

[37] W. Blanc, Z. Lu, T. Robine, F. Pigeonneau, C. Molardi, D. Tosi, Nanoparticles in optical fiber, issue and opportunity of light scattering, Opt. Mater. Express 12 (7) (2022 Jul 1) 2635–2652.

[38] Z. Lu, N. Vakula, M. Ude, M. Cabié, T. Neisius, F. Orange, F. Pigeonneau, L. Petit, W. Blanc, YbPO4 crystals in as-drawn silica-based optical fibers, Opt. Mater. 138 (2023 Apr 1) 113644.

[39] P. Vařák, M. Kamrádek, J. Aubrecht, O. Podrazký, J. Mrázek, I. Bartoň, A. Michalcová, M. Franczyk, R. Buczyński, I. Kašík, P. Peterka, Heat treatment and fiber drawing effect on the matrix structure and fluorescence lifetime of Er- and Tm-doped silica optical fibers, Opt. Mater. Express 14 (4) (2024 Apr 1) 1048–1061.

[40] H. Fneich, M. Vermillac, D.R. Neuville, W. Blanc, A. Mehdi, Highlighting of LaF3 reactivity with SiO2 and GeO2 at high temperature, Ceramics 5 (2) (2022 May 6) 182–200.

[41] M.A. Cahoon, B. Meehan, T.W. Hawkins, C. McMillen, P. Antonick, R.E. Riman, P. D. Dragic, M.J. Digonnet, J. Ballato, On the evolution of nanoparticles in nanoparticle-doped optical fibers, Opt. Mater. X 16 (2022 Oct 1) 100202.

[42] V. Fuertes, N. Grégoire, P. Labranche, S. Gagnon, N. Hamada, B. Bellanger, Y. Ledemi, S. LaRochelle, Y. Messaddeq, Cubic-shaped and rod-shaped YPO4 nanocrystal-doped optical fibers: implications for next generation of fiber lasers, ACS Appl. Nano Mater. 6 (6) (2023 Mar 14) 4337–4348.

[43] T. Cheng, M. Liao, X. Xue, J. Li, W. Gao, X. Li, D. Chen, S. Zheng, Y. Pan, T. Suzuki, Y. Ohishi, A silica optical fiber doped with yttrium aluminosilicate nanoparticles for supercontinuum generation, Opt. Mater. 53 (2016 Mar 1) 39–43.

[44] M. Vermillac, J.F. Lupi, F. Peters, M. Cabie, P. Vennegues, C. Kucera, T. Neisius, J. Ballato, W. Blanc, Fiber-draw-induced elongation and break-up of particles inside the core of a silica-based optical fiber, J. Am. Ceram. Soc. 100 (5) (2017 May) 1814–1819.

[45] Z. Lu, T. Robine, M. Guzik, M. Bellec, D. Tosi, C. Molardi, F. Pigeonneau, W. Blanc, Shaping nanoparticles in optical fibers through thermal engineering, Fiber Lasers Glass Photon.: Mater. Appl. III 12142 (2022 May 25) 81–86 (SPIE).

[46] B.N. Samson, P.A. Tick, N.F. Borrelli, Efficient neodymium-doped glass-ceramic fiber laser and amplifier, Opt Lett. 26 (3) (2001 Feb 1) 145–147.

[47] S. Yoo, U.C. Paek, W.T. Han, Development of a glass optical fiber containing ZnO–Al2O3–SiO2 glass-ceramics doped with Co2+ and its optical absorption characteristics, J. Non-Cryst. Solids 315 (1–2) (2003 Jan 1) 180–186.

[48] A. Le Sauze, C. Simonneau, A. Pastouret, D. Gicquel, L. Bigot, S. Choblet, A. M. Jurdyc, B. Jacquier, D. Bayart, L. Gasca, Nanoparticle Doping Process: towards a better control of erbium incorporation in MCVD fibers for optical amplifiers, in: Optical Amplifiers and Their Applications, Optica Publishing Group, 2003 Jul 6, p. WC5.

[49] O. Podrazky, I. Kasik, M. Pospisilova, V. Matejec, Use of alumina nanoparticles for preparation of erbium-doped fibers, LEOS 2007-IEEE Lasers Electro-Opt. Soc. Ann. Meet. Conf. Proc. 21 (2007 Oct) 246–247 (IEEE).

[50] A. Pastouret, C. Gonnet, C. Collet, O. Cavani, E. Burov, C. Chaneac, A. Carton, J. P. Jolivet, Nanoparticle doping process for improved fibre amplifiers and lasers, Fiber lasers VI: Technol. Syst., Appl. 7195 (2009 Feb 19) 449–456 (SPIE).

[51] D. Boivin, A. Pastouret, E. Burov, C. Gonnet, O. Cavani, S. Lempereur, P. Sillard, C. Goldmann, E. Saudry, C. Chanéac, A. Shlifer, Core-shell nanoparticle erbium-doped fibers for next generation amplifiers, Fiber Lasers IX: Technol. Syst. Appl. 8237 (2012 Feb 15) 457–463 (SPIE).

[52] C. Kucera, B. Kokuoz, D. Edmondson, D. Griese, M. Miller, A. James, W. Baker, J. Ballato, Designer emission spectra through tailored energy transfer in nanoparticle-doped silica preforms, Opt Lett. 34 (15) (2009 Aug 1) 2339–2341.

[53] C.J. Kucera, T.L. James, A. James, J. Ballato, Tailoring rare-earth emission spectra through controlled energy transfer, in: Optical Fiber Communication Conference, Optica Publishing Group, 2010 Mar 21, p. OThI1.

[54] C.C. Baker, E.J. Friebele, A.A. Burdett, D.L. Rhonehouse, J. Fontana, W. Kim, S. R. Bowman, L.B. Shaw, J. Sanghera, J. Zhang, R. Pattnaik, M. Dubinakii, J. Ballato, C. Kucera, A. Vargas, A. Hemming, N. Simakov, J. Haub, Nanoparticle doping for high power fiber lasers at eye-safer wavelengths, Opt Express 25 (12) (2017 Jun 12) 13903–13915.

[55] J.R. DiMaio, B. Kokuoz, J. Ballato, Ultra-broadband amplification through nanotechnology, Active Passive Opt. Components Commun. VI 6389 (2006 Oct 2) 56–65 (SPIE).

[56] F. d'Acapito, C. Maurizio, M.C. Paul, T.S. Lee, W. Blanc, B. Dussardier, Role of CaO addition in the local order around Erbium in SiO2–GeO2–P2O5 fiber preforms, Mater. Sci. Eng. B 146 (1–3) (2008 Jan 15) 167–170.

[57] W. Blanc, B. Dussardier, M.C. Paul, Er doped oxide nanoparticles in silica based optical fibres, Glass Technol. Eur. J. Glass Sci. Technol. 50 (1) (2009 Feb 14) 79–81.

[58] D. Boivin, T. Föhn, E. Burov, A. Pastouret, C. Gonnet, O. Cavani, C. Collet, S. Lempereur, Quenching investigation on new erbium doped fibers using MCVD nanoparticle doping process, Fiber Lasers VII: Technol. Syst. Appl. 7580 (2010 Feb 17) 627–635 (SPIE).

[59] M.C. Paul, S.W. Harun, N.A. Huri, A. Hamzah, S. Das, M. Pal, S.K. Bhadra, H. Ahmad, S. Yoo, M.P. Kalita, A.J. Boyland, Wideband EDFA based on erbium doped crystalline zirconia yttria alumino silicate fiber, J. Lightwave Technol. 28 (20) (2010 Oct 15) 2919–2924.

[60] M.C. Paul, S. Bysakh, S. Das, S.K. Bhadra, M. Pal, S. Yoo, M.P. Kalita, A. J. Boyland, J.K. Sahu, Yb2O3-doped YAG nano-crystallites in silica-based core glass matrix of optical fiber preform, Mater. Sci. Eng. B 175 (2) (2010 Nov 25) 108–119.

[61] G. Brasse, C. Restoin, J.L. Auguste, S. Hautreux, J.M. Blondy, A. Lecomte, Nanostructured optical fiber by the sol-gel process in the SiO2–ZrO2 system, Appl. Phys. Lett. 91 (12) (2007 Sep 17).

[62] G. Brasse, C. Restoin, J.L. Auguste, S. Hautreux, J.M. Blondy, F. Sandoz, C. Pedrido, Nanoscaled optical fibre obtained by the sol–gel process in the SiO2–ZrO2 system doped with rare earth ions, Opt. Mater. 31 (5) (2009 Mar 1) 765–768.

[63] Kamrádek M. Nanoparticles-doped silica-glass-based optical fibers: fabrication and application. In Specialty Opt. Fib. 2024 Jan 1 (pp. 159-181). (Woodhead Publishing).

[64] Wang W, Zhang Q. Fabrication and applications of nanostructured soft-glass optical fiber. In Specialty Opt. Fib. 2024 Jan 1 (pp. 127-158). (Woodhead Publishing).

[65] W. Blanc, B. Dussardier, Formation and applications of nanoparticles in silica optical fibers, J. Opt. 45 (3) (2016 Sep) 247–254.

[66] M.C. Paul, S. Bysakh, S. Das, A. Dhar, M. Pal, S.K. Bhadra, J.K. Sahu, A. V. Kir'yanov, F. d'Acapito, Recent developments in rare-earths doped nano-engineered glass based optical fibers for high power fiber lasers, Trans. Indian Ceram. Soc. 75 (4) (2016 Oct 1) 195–208.

[67] A. Veber, Z. Lu, M. Vermillac, F. Pigeonneau, W. Blanc, L. Petit, Nano-structured optical fibers made of glass-ceramics, and phase separated and metallic particle-containing glasses, Fibers 7 (12) (2019 Nov 30) 105.

[68] Z. Zhu, S. Sun, X. Chai, J. Gao, M. Lu, Z. Wu, Y. Gao, T. Feng, X. Bai, Y. Zhang, F. Yan, Quantum dot-doped optical fibers, Laser Photon. Rev. (2024 May 5) 2301388.

[69] S. Ju, V.L. Nguyen, P.R. Watekar, B.H. Kim, C. Jeong, S. Boo, C.J. Kim, W.T. Han, Fabrication and optical characteristics of a novel optical fiber doped with the Au nanoparticles, J. Nanosci. Nanotechnol. 6 (11) (2006 Nov 1) 3555–3558.

[70] F. Pang, X. Zeng, Z. Chen, T. Wang, Fabrication and characteristics of silica optical fiber doped with InP nano-semiconductor material, Opt. Quant. Electron. 39 (2007 Oct) 975–981.

[71] B.J. Ainslie, H.P. Girdlestone, D. Cotter, Semiconductor-doped fibre waveguides exhibiting picosecond optical nonlinearity, Electron. Lett. 23 (8) (1987 Apr 9) 405–406.

[72] D. Cotter, C.N. Ironside, B.J. Ainslie, H.P. Girdlestone, Picosecond pump–probe interferometric measurement of optical nonlinearity in semiconductor-doped fibers, Opt Lett. 14 (6) (1989 Mar 15) 317–319.

[73] A. Lizuka, K. Ogura, Optical fiber provided with optical non-linear characteristic, Japan. Patent Appl. JPH04195028A (1990 Nov 28).

[74] M.G. Burt, Optical fibre with quantum dots, United States Patent US 5 (881,200. 1999 Mar 9).

[75] S. Moon, B.H. Kim, P.R. Watekar, W.T. Han, Fabrication and photoluminescence characteristics of Er3+-doped optical fibre sensitised by silicon, Electron. Lett. 43 (2) (2007 Jan 18) 85–87.

[76] A. Lin, D.H. Son, I.H. Ahn, G.H. Song, W.T. Han, Visible to infrared photoluminescence from gold nanoparticles embedded in germano-silicate glass fiber, Opt Express 15 (10) (2007 May 14) 6374–6379.

[77] P.R. Watekar, A. Lin, S. Ju, W.T. Han, 1537 nm emission upon 980 nm pumping in PbSe quantum dots doped optical fiber, in: OFC/NFOEC 2008-2008 Conference on Optical Fiber Communication/National Fiber Optic Engineers Conference, 2008 Feb 24, pp. 1–3 (IEEE).

[78] A. Lin, P.R. Watekar, G. Sun, Y. Chung, W.T. Han, Linear and resonant nonlinear optical properties of Ag-nanocrystals incorporated germano-silicate fiber, in: OFC/NFOEC 2008-2008 Conference on Optical Fiber Communication/National Fiber Optic Engineers Conference, 2008 Feb 24, pp. 1–3 (IEEE).

[79] W. Blanc, B. Dussardier, G. Monnom, R. Peretti, A.M. Jurdyc, B. Jacquier, M. Foret, A. Roberts, Erbium emission properties in nanostructured fibers, Appl. Opt. 48 (31) (2009 Nov 1) G119–G124.

[80] S. Ju, P.R. Watekar, W.T. Han, Fabrication of highly nonlinear germano-silicate glass optical fiber incorporated with PbTe semiconductor quantum dots using atomization doping process and its optical nonlinearity, Opt Express 19 (3) (2011 Jan 31) 2599–2607.

[81] D. Boivin, A. Pastouret, E. Burov, C. Gonnet, O. Cavani, S. Lempereur, P. Sillard, Performance characterization of new erbium-doped fibers using MCVD nanoparticle doping process, Fiber Lasers VIII: Technol. Syst. Appl. 7914 (2011 Feb 10) 475–485 (SPIE).

[82] A.V. Kir'yanov, M.C. Paul, Y.O. Barmenkov, S. Das, M. Pal, S.K. Bhadra, L. E. Zarate, A.D. Guzman-Chavez, Fabrication and characterization of new Yb-doped zirconia-germano-alumino silicate phase-separated nano-particles based fibers, Opt Express 19 (16) (2011 Aug 1) 14823–14837.

[83] J. Thomas, M. Myara, L. Troussellier, E. Burov, A. Pastouret, D. Boivin, G. Mélin, O. Gilard, M. Sotom, P. Signoret, Radiation-resistant erbium-doped-nanoparticles optical fiber for space applications, Opt Express 20 (3) (2012 Jan 30) 2435–2444.

[84] A. Dhar, I. Kasik, B. Dussardier, O. Podrazky, V. Matejec, Preparation and properties of Er-doped ZrO2 nanocrystalline phase-separated preforms of optical fibers by MCVD process, Int. J. Appl. Ceram. Technol. 9 (2) (2012 Mar) 341–348.

[85] M.C. Paul, A.V. Kir'Yanov, Y.O. Barmenkov, S. Das, M. Pal, S.K. Bhadra, S. Yoo, A. J. Boyland, J.K. Sahu, A. Martinez-Gamez, J.L. Lucio-Martínez, Yb2O3 doped

yttrium-alumino-silicate nano-particles based LMA optical fibers for high-power fiber lasers, J. Lightwave Technol. 30 (13) (2012 Apr 3) 2062–2068.
[86] T. Lindstrom, E. Garber, D. Edmonson, T. Hawkins, Y. Chen, G. Turri, M. Bass, J. Ballato, Spectral engineering of optical fiber preforms through active nanoparticle doping, Opt. Mater. Express 2 (11) (2012 Nov 1) 1520–1528.
[87] W. Blanc, C. Guillermier, B. Dussardier, Composition of nanoparticles in optical fibers by secondary ion mass spectrometry, Opt. Mater. Express 2 (11) (2012 Nov 1) 1504–1510.
[88] A. Dhar, I. Kasik, O. Podrazky, V. Matejec, Fabrication and properties of Er-doped nanocrystalline phase-separated optical fibers, Adv. Electric. Electr. Eng. 11 (1) (2013 Mar 30) 29–35.
[89] I. Kasik, O. Podrazky, J. Mrazek, J. Cajzl, J. Aubrecht, J. Probostova, P. Peterka, P. Honzatko, A. Dhar, Erbium and Al2O3 nanocrystals-doped silica optical fibers, Bull. Pol. Acad. Sci. Tech. Sci. 62 (4) (2014 Oct) 641–646.
[90] F. d'Acapito, W. Blanc, B. Dussardier, Different Er3+ environments in Mg-based nanoparticle-doped optical fibre preforms, J. Non-Cryst. Solids 401 (2014 Oct 1) 50–53.
[91] J. Mrazek, I. Kasik, L. Prochazkova, V. Cuba, J. Aubrecht, J. Cajzl, O. Podrazky, P. Peterka, M. Nikl, Active optical fibers doped with ceramic nanocrystals, Adv. Electric. Electr. Eng. 12 (6) (2014 Dec 30) 567–574.
[92] M.C. Paul, A. Dhar, S. Das, A.A. Latiff, M.T. Ahmad, S.W. Harun, Development of nanoengineered thulium-doped fiber laser with low threshold pump power and tunable operating wavelength, IEEE Photon. J. 7 (1) (2015 Feb 2) 1–8.
[93] Y. Dong, J. Wen, F. Pang, Y. Luo, G.D. Peng, Z. Chen, T. Wang, Formation and photoluminescence property of PbS quantum dots in silica optical fiber based on atomic layer deposition, Opt. Mater. Express 5 (4) (2015 Apr 1) 712–719.
[94] I. Savelii, L. Bigot, H. El Hamzaoui, G. Bouwmans, S. Plus, B. Capoen, A. M. Blanchenet, A. Pastouret, C. Chanéac, M. Bouazaoui, Evidence of Yb-to-Er energy transfer in AlPO4: Yb3+/Er3+ nanoparticle-doped silica optical fiber preform, in: The European Conference on Lasers and Electro-Optics, Optica Publishing Group, 2015 Jun 21 (p. CE_1_1).
[95] C.C. Baker, E.J. Friebele, C.G. Askins, J.P. Fontana, M.P. Hunt, J.R. Peele, B. A. Marcheschi, W. Kim, J. Sanghera, J. Zhang, R.K. Pattnaik, Erbium nanoparticle doping for high power fiber lasers, Novel Opt. Mater. Appl. 27 (2015 Jun) NS2A–3 (Optica Publishing Group).
[96] C.C. Baker, E.J. Friebele, C.G. Askins, M.P. Hunt, B.A. Marcheschi, J. Fontana, J. R. Peele, W. Kim, J. Sanghera, J. Zhang, R.K. Pattnaik, Nanoparticle doping for improved Er-doped fiber lasers, Fiber Lasers XIII: Technol. Syst. Appl. 9728 (2016 Mar 16) 170–178 (SPIE).
[97] F. Qin, Y. Dong, J. Wen, F. Pang, Y. Luo, G.D. Peng, Z. Chen, T. Wang, Effect of heat treatment on absorption and fluorescence properties of PbS-doped silica optical fibre, Opt. Mater. 64 (2017 Feb 1) 468–473.
[98] E.J. Friebele, C.C. Baker, A.A. Burdett, D.L. Rhonehouse, S.R. Bowman, W. Kim, J. S. Sanghera, C. Kucera, A. Vargas, J. Ballato, A. Hemming, Ho-nanoparticle-doping for improved high-energy laser fibers, Opt. Component Mater. XIV 10100 (2017 Mar 7) 20–25 (SPIE).
[99] M. Vermillac, H. Fneich, J.F. Lupi, J.B. Tissot, C. Kucera, P. Vennéguès, A. Mehdi, D.R. Neuville, J. Ballato, W. Blanc, Use of thulium-doped LaF3 nanoparticles to lower the phonon energy of the thulium's environment in silica-based optical fibres, Opt. Mater. 68 (2017 Jun 1) 24–28.
[100] Y. Shang, J. Wen, Y. Dong, H. Zhan, Y. Luo, G.D. Peng, X. Zhang, F. Pang, Z. Chen, T. Wang, Luminescence properties of PbS quantum-dot-doped silica optical fibre produced via atomic layer deposition, J. Lumin. 187 (2017 Jul 1) 201–204.
[101] Vermillac M, Lupi JF, Fneich H, Turlier J, Cabié M, Kucera C, Borschneck D, Peters F, Chaussedent S, Vennegues P, Neuville DR. Thulium-doped nanoparticles and their properties in silica-based optical fibers. In Fiber Lasers Glass Photon.: Mater. Appl. 2018 May 17 (Vol. 10683, pp. 199-207). (SPIE).
[102] J. Mrázek, I. Kašík, L. Procházková, V. Čuba, V. Girman, V. Puchý, W. Blanc, P. Peterka, J. Aubrecht, J. Cajzl, O. Podrazký, YAG ceramic nanocrystals implementation into MCVD technology of active optical fibers, Appl. Sci. 8 (5) (2018 May 21) 833.
[103] J. Cajzl, P. Peterka, M. Kowalczyk, J. Tarka, G. Sobon, J. Sotor, J. Aubrecht, P. Honzátko, I. Kašík, Thulium-doped silica fibers with enhanced fluorescence lifetime and their application in ultrafast fiber lasers, Fibers 6 (3) (2018 Sep 16) 66.
[104] M. Paul, A. Kir'yanov, Y. Barmenkov, M. Pal, R. Youngman, A. Dhar, S. Das, Phase-separated alumina–silica glass-based erbium-doped fibers for optical amplifier: material and optical characterization along with amplification properties, Fibers 6 (3) (2018 Sep 17) 67.
[105] Pan X, Dong Y, Wen J, Huang Y, Deng C, Wang T. Highly sensitive temperature sensor of fiber Bragg grating on PbS-doped silica optical fiber. In Optical Fiber Sensors 2018 Sep 24 (p. ThE1). Optica Publishing Group.
[106] J. Zhang, C.C. Baker, R. Pattnaik, E.J. Friebele, A. Burdett, D.L. Rhonehouse, W. Kim, J. Sanghera, M. Dubinskii, High power resonantly-diode-pumped fiber laser based on Er-Nanoparticle-Doped fiber, Adv. Solid State Lasers 4 (2018 Nov) AM5A, 1). Optica Publishing Group.
[107] M. Vermillac, H. Fneich, J. Turlier, M. Cabié, C. Kucera, D. Borschneck, F. Peters, P. Vennéguès, T. Neisius, S. Chaussedent, D.R. Neuville, On the morphologies of oxides particles in optical fibers: effect of the drawing tension and composition, Opt. Mater. 87 (2019 Jan 1) 74–79.
[108] M. Kamrádek, I. Kašík, J. Aubrecht, J. Mrázek, O. Podrazký, J. Cajzl, P. Vařák, V. Kubeček, P. Peterka, P. Honzátko, Nanoparticle and solution doping for efficient holmium fiber lasers, IEEE Photon. J. 11 (5) (2019 Sep 11) 1, 0.
[109] X. Pan, Y. Dong, J. Zheng, J. Wen, F. Pang, Z. Chen, Y. Shang, T. Wang, Enhanced FBG temperature sensitivity in PbS-doped silica optical fiber, J. Lightwave Technol. 37 (18) (2019 Sep 15) 4902–4907.
[110] W. Blanc, Z. Lu, M. Vermillac, J. Fourmont, I. Martin, H.F. Saint-Cyr, C. Molardi, D. Tosi, A. Piarresteguy, F. Mady, M. Benabdesselam, Reconsidering nanoparticles in optical fibers, Opt. Component Mater. XVII 11276 (2020 Mar 3) 148–154 (SPIE).
[111] A. Mansoor, S.H. Heder, S.Z. Muhd-Yasin, M.C. Paul, Z. Yusuff, H.A. Abdul-Rashid, Compact thulium fiber amplifier codoped with yttria nano-particle operating at 1800nm region, in: 2020 IEEE 8th International Conference on Photonics (ICP), IEEE, 2020 May 12, pp. 52–53.
[112] S. Jagannathan, Low Threshold Random Lasing from Phase Separated Optical Fibers (Doctoral Dissertation, University of Illinois at Urbana-Champaign, May 2020.
[113] P. Vařák, J. Mrázek, W. Blanc, J. Aubrecht, M. Kamrádek, O. Podrazký, Preparation and properties of Tm-doped SiO2-ZrO2 phase separated optical fibers for use in fiber lasers, Opt. Mater. Express 10 (6) (2020 Jun 1) 1383–1391.
[114] S. Jagannathan, L. Ackerman, W. Chen, N. Yu, M. Cavillon, M. Tuggle, T. W. Hawkins, J. Ballato, P.D. Dragic, Random lasing from optical fibers with phase separated glass cores, Opt Express 28 (15) (2020 Jul 20) 22049–22063.
[115] Vařák P, Mrázek J, Blanc W, Aubrecht J, Kamrádek M, Podrazký O, Honzátko P. Nanocrystalline ZrO2-doped active optical fibers for fiber lasers operating at 2 μm. In Micro-struct. Specialty Opt. Fib. VII 2021 Apr 18 (Vol. 11773, pp. 184-190). (SPIE).
[116] Y.W. Lee, J.Y. Chuang, C.C. Lin, M.C. Paul, S. Das, A. Dhar, High-efficiency picosecond mode-locked laser using a thulium-doped nanoengineered yttrium-alumina-silica fiber as the gain medium, Opt Express 29 (10) (2021 May 10) 14682–14693.
[117] M. Cabié, T. Neisius, W. Blanc, Combined FIB/SEM tomography and TEM analysis to characterize high aspect ratio Mg-silicate particles inside silica-based optical fibres, Mater. Char. 178 (2021 Aug 1) 111261.
[118] P. Vařák, J. Mrázek, A.A. Jasim, S. Bysakh, A. Dhar, M. Kamrádek, O. Podrazký, I. Kašík, I. Bartoň, P. Nekvindová, Thermal stability and photoluminescence properties of RE-doped (RE= Ho, Er, Tm) alumina nanoparticles in bulk and fiber-optic silica glass, Opt. Mater. 118 (2021 Aug 1) 111239.
[119] Y. Dong, Y. Zhao, H. Zhang, J. Wen, X. Zhang, Y. Huang, Y. Shang, H. Wei, T. Wang, Theoretical study on ultra-broadband gain and low noise characteristics of PbS quantum dots-doped silica fiber amplifier, Opt Commun. 493 (2021 Aug 15) 126992.
[120] P. Vařák, I. Kašík, M. Kamrádek, O. Podrazký, J. Mrázek, P. Peterka, R. Buczynski, M. Franczyk, P. Honzátko, Heat treatment and fiber drawing effect on the fluorescence lifetime of re3+-doped preforms and fibers, in: Laser Applications Conference, Optica Publishing Group, 2021 Oct 3, pp. JTu1A–38.
[121] Vigneron PB, Meehan B, Cahoon MA, Hawkins TW, Ballato JM, Dragic PD, Engholm M, Boilard T, Bernier M, Digonnet MJ. Anti-Stokes cooling in silica and nanoparticle-doped silicate fibers. In Photon. Heat Eng.: Sci. Appl. IV 2022 Mar 3 (Vol. 12018, pp. 45-52). (SPIE).
[122] Thomas J, Meyneng T, Tehranchi A, Manarazan P, Monet F, Boisvert JS, Morency S, Grégoire N, Seletskiy D, Messaddeq Y, Kashyap R. Characteristics of Yb-doped silica fibers containing Y2O3 nanoparticles for optical refrigeration. In Photon. Heat Eng.: Sci. Appl. IV 2022 Mar 3 (Vol. 12018, pp. 53-57). (SPIE).
[123] Vařák P, Kašík I, Peterka P, Mrázek J, Kamrádek M, Aubrecht J, Podrazký O, Bartoň I, Franczyk M, Buczynski R, Honzátko P. The effect of thermal and mechanical processing on the fluorescence lifetime of Yb-doped silica preforms and fibers for use in nanostructured-core fiber lasers. In Fiber Lasers XIX: Technol. Syst. 2022 Mar 4 (Vol. 11981, pp. 5-10). (SPIE).
[124] V. Fuertes, N. Grégoire, S. Morency, S. Gagnon, Y. Ledemi, S. LaRochelle, Y. Messaddeq, Tunable distributed sensing performance in Ca-based nanoparticle-doped optical fibers, Opt. Mater. Express 12 (4) (2022 Apr 1) 1323–1336.
[125] P. Vařák, I. Kašík, P. Peterka, J. Aubrecht, J. Mrázek, M. Kamrádek, O. Podrazký, I. Bartoň, M. Franczyk, R. Buczynski, P. Honzátko, Heat treatment and fiber drawing effect on the luminescence properties of RE-doped optical fibers (RE= Yb, Tm, Ho), Opt. Expr. 30 (6) (2022 Mar 14) 10050–10062.
[126] P.B. Vigneron, B. Meehan, M.A. Cahoon, T.W. Hawkins, J. Ballato, P.D. Dragic, M. Engholm, T. Boilard, M. Bernier, M.J. Digonnet, Anti-Stokes fluorescence cooling of nanoparticle-doped silica fibers, Opt Lett. 47 (10) (2022 May 15) 2590–2593.
[127] J. Fourmont, W. Blanc, D. Guichaoua, S. Chaussedent, Phase-separated Ca and Mg-based nanoparticles in SiO2 glass investigated by molecular dynamics simulations, Sci. Rep. 12 (1) (2022 Jul 13) 11959.
[128] J. Luo, X. Zhang, S. Yang, W. Blanc, Z. Yan, X. Yu, Narrow linewidth fiber laser based on nanoparticles doped self-injection module, in: 2022 Asia Communications and Photonics Conference (ACP), 2022 Nov 5, pp. 202–206 (IEEE).
[129] J. Thomas, T. Meyneng, A. Tehranchi, N. Gregoire, F. Monet, D. Seletskiy, Y. Messaddeq, R. Kashyap, Demonstration of laser cooling in a novel all oxide GAYY silica glass, Sci. Rep. 13 (1) (2023 Apr 3) 5436.
[130] J. Luo, X. Zhang, S. Yang, W. Blanc, Z. Yan, X. Yu, Sub-kilohertz narrow linewidth fiber laser based on nanoparticles doped self-injection module, IEEE Photon. Technol. Lett. 35 (2023 Apr 5) 613–616. Issue: 11, 01 June 2023) Page(s).
[131] T. Meyneng, J. Thomas, N. Grégoire, W. Leelapornpisit, J. Valdez, R. Kashyap, Y. Messaddeq, Controlled phase-separation effect for enhanced optical refrigeration in yttrium-aluminosilicate glasses, J. Mater. Chem. C 11 (23) (2023 May 17) 7619–7628.
[132] V. Fuertes, N. Grégoire, P. Labranche, S. Gagnon, S. LaRochelle, Y. Messaddeq, Towards REPO4 nanocrystal-doped optical fibers for distributed sensing applications, Sci. Rep. 13 (1) (2023 Aug 9) 12891.
[133] J. Thomas, T. Meyneng, A. Tehranchi, N. Gregoire, V. Karpov, D. Seletskiy, Y. Messaddeq, R. Kashyap, Anti-Stokes cooling in highly ytterbium doped phase

separated aluminium-yttrium oxide glass by 4 k, Opt. Mater. 144 (2023 Oct 1) 114374.
[134] V. Fuertes, N. Grégoire, P. Labranche, S. Gagnon, N. Hamada, S. LaRochelle, Y. Messaddeq, In situ crystallization of SiO spherical nanocrystals in optical fibers, J. Non-Cryst. Solids 621 (2023 Dec 1) 122640.
[135] P. Vařák, M. Kamrádek, J. Aubrecht, O. Podrazký, J. Mrázek, I. Bartoň, A. Michalcová, M. Franczyk, R. Buczyński, I. Kašík, P. Peterka, Heat treatment and fiber drawing effect on the matrix structure and fluorescence lifetime of Er- and Tm-doped silica optical fibers, Opt. Mater. Express 14 (4) (2024 Apr 1) 1048–1061.
[136] J. Campbell, M.A. Cahoon, M. Gachich, M. Norlander, T. Hawkins, J. Ballato, P. Dragic, Gain optimization of Er-doped fibers doped with Er:BaF2 nanoparticles, 2024 Opt. Fiber Commun. Conf. Exhibit. (OFC) 24 (2024 Mar) 1–3 (IEEE).
[137] J. Lee, M.A. Cahoon, B. Meehan, Y. Ososkov, T.W. Hawkins, J. Ballato, S. D. Jackson, Visible silica fiber laser based on Dy: BaF2 nanoparticle doping, Opt. Mater. Express 14 (8) (2024 Jul 23) 2023–2031.
[138] G. Pickrell, N. Manjooran, N. Goel, D. Kominsky, Silicon induced *in situ* hole formation in optical fibers, J. Non-Cryst. Solids 352 (6–7) (2006 May 15) 500–504.
[139] D. Dorosz, M. Kochanowicz, R. Valiente, A. Diego-Rucabado, F. Rodríguez, N. Siñeriz-Niembro, J.I. Espeso, M. Lesniak, P. Miluski, S. Conzendorf, J. Posseckardt, Pr3+-doped YPO4 nanocrystal embedded into an optical fiber, Sci. Rep. 14 (1) (2024 Mar 28) 7404.
[140] Z. Fang, S. Zheng, W. Peng, H. Zhang, Z. Ma, G. Dong, S. Zhou, D. Chen, J. Qiu, Ni2+ doped glass ceramic fiber fabricated by melt-in-tube method and successive heat treatment, Opt Express 23 (22) (2015 Nov 2) 28258–28263.
[141] S.N.B. Bhaktha, P. Sebbah, W. Blanc, B. Dussardier, M. Ude, S. Trzesien, Spectroscopic characterizations of nanostructured Er3+-doped optical fibers: towards the development of a fibre random laser, Poster 7713-62 SPIE Photon. Eur. Brussels, Belgium, April 12–16 (2010).
[142] Y. Wang, H. Yuan, X. Liu, Q. Bai, H. Zhang, Y. Gao, B. Jin, A comprehensive study of optical fiber acoustic sensing, IEEE Access 7 (2019 Jun 24) 85821–85837.
[143] C. Broadway, R. Min, A.G. Leal-Junior, C. Marques, C. Caucheteur, Toward commercial polymer fiber Bragg grating sensors: review and applications, J. Lightwave Technol. 37 (11) (2019 Jun 1) 2605–2615.
[144] A. Ukil, H. Braendle, P. Krippner, Distributed temperature sensing: review of technology and applications, IEEE Sensor. J. 12 (5) (2011 Jul 18) 885–892.
[145] X. Bao, L. Chen, Recent progress in distributed fiber optic sensors, Sensors 12 (7) (2012 Jun 26) 8601–8639.
[146] M. Froggatt, J. Moore, High-spatial-resolution distributed strain measurement in optical fiber with Rayleigh scatter, Appl. Opt. 37 (10) (1998 Apr 1) 1735–1740.
[147] Z. Ding, C. Wang, K. Liu, J. Jiang, D. Yang, G. Pan, Z. Pu, T. Liu, Distributed optical fiber sensors based on optical frequency domain reflectometry: a review, Sensors 18 (4) (2018 Apr 3) 1072.
[148] Y. Du, S. Jothibasu, Y. Zhuang, C. Zhu, J. Huang, Unclonable optical fiber identification based on Rayleigh backscattering signatures, J. Lightwave Technol. 35 (21) (2017 Sep 19) 4634–4640.
[149] L. Schenato, M. Cappelletti, D. Orsuti, A. Galtarossa, M. Santagiustina, S. Cola, L. Palmieri, Long-term persistence of Rayleigh signature of optical fibers in harsh environment, J. Lightwave Technol. 42 (18) (2024 Jun 13) 6254–6261.
[150] L. Schenato, A review of distributed fibre optic sensors for geo-hydrological applications, Appl. Sci. 7 (9) (2017 Sep 1) 896.
[151] A. Yan, S. Huang, S. Li, R. Chen, P. Ohodnicki, M. Buric, S. Lee, M.J. Li, K.P. Chen, Distributed optical fiber sensors with ultrafast laser enhanced Rayleigh backscattering profiles for real-time monitoring of solid oxide fuel cell operations, Sci. Rep. 7 (1) (2017 Aug 24) 9360.
[152] F. Monet, S. Loranger, V. Lambin-Iezzi, A. Drouin, S. Kadoury, R. Kashyap, The ROGUE: a novel, noise-generated random grating, Opt Express 27 (10) (2019 May 13) 13895–13909.
[153] A. Dostovalov, A. Wolf, Z. Munkueva, M. Skvortsov, S. Abdullina, A. Kuznetsov, S. Babin, Continuous and discrete-point Rayleigh reflectors inscribed by femtosecond pulses in singlemode and multimode fibers, Opt Laser. Technol. 167 (2023 Dec 1) 109692.
[154] S. Loranger, M. Gagné, V. Lambin-Iezzi, R. Kashyap, Rayleigh scatter based order of magnitude increase in distributed temperature and strain sensing by simple UV exposure of optical fibre, Sci. Rep. 5 (1) (2015 Jun 16) 11177.
[155] I. Gasulla, D. Barrera, J. Hervás, S. Sales, Spatial division multiplexed microwave signal processing by selective grating inscription in homogeneous multicore fibers, Sci. Rep. 7 (1) (2017 Jan 30) 41727.
[156] A. Beisenova, A. Issatayeva, S. Sovetov, S. Korganbayev, M. Jelbuldina, Z. Ashikbayeva, W. Blanc, E. Schena, S. Sales, C. Molardi, D. Tosi, Multi-fiber distributed thermal profiling of minimally invasive thermal ablation with scattering-level multiplexing in MgO-doped fibers, Biomed. Opt Express 10 (3) (2019 Mar 1) 1282–1296.
[157] P. Saccomandi, E. Schena, S. Silvestri, Techniques for temperature monitoring during laser-induced thermotherapy: an overview, Int. J. Hyperther. 29 (7) (2013 Nov 1) 609–619.
[158] Z. Ashikbayeva, A. Aitkulov, T.S. Atabaev, W. Blanc, V.J. Inglezakis, D. Tosi, Green-synthesized silver nanoparticle–assisted radiofrequency ablation for improved thermal treatment distribution, Nanomaterials 12 (3) (2022 Jan 27) 426.
[159] A. Sametova, S. Kurmashev, Z. Ashikbayeva, W. Blanc, D. Tosi, Optical fiber distributed sensing network for thermal mapping in radiofrequency ablation neighboring a blood vessel, Biosensors 12 (12) (2022 Dec 8) 1150.
[160] Z. Ashikbayeva, A. Aitkulov, M. Jelbuldina, A. Issatayeva, A. Beisenova, C. Molardi, P. Saccomandi, W. Blanc, V.J. Inglezakis, D. Tosi, Distributed 2D temperature sensing during nanoparticles assisted laser ablation by means of high-scattering fiber sensors, Sci. Rep. 10 (1) (2020 Jul 28) 12593.
[161] A. Beisenova, A. Issatayeva, Z. Ashikbayeva, M. Jelbuldina, A. Aitkulov, V. Inglezakis, W. Blanc, P. Saccomandi, C. Molardi, D. Tosi, Distributed sensing network enabled by high-scattering MgO-doped optical fibers for 3D temperature monitoring of thermal ablation in liver phantom, Sensors 21 (3) (2021 Jan 27) 828.
[162] A. Issatayeva, A. Amantayeva, W. Blanc, C. Molardi, D. Tosi, Temperature compensation of the fiber-optic based system for the shape reconstruction of a minimally invasive surgical needle, Sensor Actuator Phys. 329 (2021 Oct 1) 112795.
[163] A. Beisenova, A. Issatayeva, I. Iordachita, W. Blanc, C. Molardi, D. Tosi, Distributed fiber optics 3D shape sensing by means of high scattering NP-doped fibers simultaneous spatial multiplexing, Opt Express 27 (16) (2019 Aug 5) 22074–22087.
[164] A. Issatayeva, A. Amantayeva, W. Blanc, D. Tosi, C. Molardi, Design and analysis of a fiber-optic sensing system for shape reconstruction of a minimally invasive surgical needle, Sci. Rep. 11 (1) (2021 Apr 21) 8609.
[165] Z. Katrenova, S. Alisherov, M. Yergibay, Z. Kappasov, W. Blanc, D. Tosi, C. Molardi, Bite force mapping based on distributed fiber sensing network approach, Sensors 24 (2) (2024 Jan 15) 537.
[166] M. Sypabekova, A. Aitkulov, W. Blanc, D. Tosi, Reflector-less nanoparticles doped optical fiber biosensor for the detection of proteins: case thrombin, Biosens. Bioelectron. 165 (2020 Oct 1) 112365.
[167] M. Shaimerdenova, T. Ayupova, Z. Ashikbayeva, A. Bekmurzayeva, W. Blanc, D. Tosi, Reflector-less shallow-tapered optical fiber biosensors for rapid detection of cancer biomarkers, J. Lightwave Technol. 41 (13) (2023 Jul 1) 4114–4122.
[168] A. Aitkulov, M. Sypabekova, C. Molardi, W. Blanc, D. Tosi, Fabrication and performance evaluation of reflectorless refractive index fiber optic sensors using etched enhanced backscattering fibers, Measurement 172 (2021 Feb 1) 108874.
[169] M. Olivero, A. Mirigaldi, V. Serafini, A. Vallan, G. Perrone, W. Blanc, M. Benabdesselam, F. Mady, C. Molardi, D. Tosi, Distributed X-ray dosimetry with optical fibers by optical frequency domain interferometry, IEEE Trans. Instrum. Meas. 70 (2021 Apr 26) 1–9.
[170] I. Floris, J.M. Adam, P.A. Calderón, S. Sales, Fiber optic shape sensors: a comprehensive review, Opt Laser. Eng. 139 (2021 Apr 1) 106508.
[171] J. Guo, K. Zhu, Q. Wu, J. Liu, K. Yan, J. Wang, Batch fabrication of the smooth-surfaced and tailored-diameter microfiber Bragg grating sensors using hydrothermal method and its characteristics, Opt. Fiber Technol. 81 (2023 Dec 1) 103534.
[172] F. Bayle, J.P. Meunier, Efficient fabrication of fused-fiber biconical taper structures by a scanned CO 2 laser beam technique, Appl. Opt. 44 (30) (2005 Oct 20) 6402–6411.
[173] T. Guo, Á. González-Vila, M. Loyez, C. Caucheteur, Plasmonic optical fiber-grating immunosensing: a review, Sensors 17 (12) (2017 Nov 26) 2732.
[174] K. Shafique, B.A. Khawaja, F. Sabir, S. Qazi, M. Mustaqim, Internet of things (IoT) for next-generation smart systems: a review of current challenges, future trends and prospects for emerging 5G-IoT scenarios, IEEE Access 8 (2020 Jan 28) 23022–23040.
[175] Z.M. Hira, D.F. Gillies, A review of feature selection and feature extraction methods applied on microarray data, Adv. Bioinform. 2015 (1) (2015) 198363.
[176] C. Garrido-Hidalgo, D. Hortelano, L. Roda-Sanchez, T. Olivares, M.C. Ruiz, V. Lopez, IoT heterogeneous mesh network deployment for human-in-the-loop challenges towards a social and sustainable Industry 4.0, IEEE Access 6 (2018 May 21) 28417–28437.
[177] Y. Zhou, Y.N. Zhang, Q. Yu, L. Ren, Q. Liu, Y. Zhao, Application of machine learning in optical fiber sensors, Measurement (2024 Feb 23) 114391.
[178] E. Reyes-Vera, A. Valencia-Arias, V. García-Pineda, E.F. Aurora-Vigo, H. Alvarez Vásquez, G. Sánchez, Machine learning applications in optical fiber sensing: a research agenda, Sensors 24 (7) (2024 Mar 29) 2200.
[179] L. Chen, Y.K. Leng, B. Liu, J. Liu, S.P. Wan, T. Wu, J. Yuan, L. Shao, G. Gu, Y. Q. Fu, H. Xu, Ultrahigh-sensitivity label-free optical fiber biosensor based on a tapered singlemode-no core-singlemode coupler for Staphylococcus aureus detection, Sensor. Actuator. B Chem. 320 (2020 Oct 1) 128283.
[180] L. Avellar, C. Stefano Filho, G. Delgado, A. Frizera, E. Rocon, A. Leal-Junior, AI-enabled photonic smart garment for movement analysis, Sci. Rep. 12 (1) (2022 Mar 8) 4067.
[181] Z. Ding, C. Wang, K. Liu, J. Jiang, D. Yang, G. Pan, Z. Pu, T. Liu, Distributed optical fiber sensors based on optical frequency domain reflectometry: a review, Sensors 18 (4) (2018 Apr 3) 1072.
[182] N. Arandia, J.I. Garate, J. Mabe, Embedded sensor systems in medical devices: requisites and challenges ahead, Sensors 22 (24) (2022 Dec 16) 9917.
[183] R. Diaz Ca, A.G. Leal-Junior, M. Avellar L, C. Antunes Pf, M.J. Pontes, C. A. Marques, A. Frizera, N. Ribeiro MR. Perrogator, A portable energy-efficient interrogator for dynamic monitoring of wavelength-based sensors in wearable applications, Sensors 19 (13) (2019 Jul 5) 2962.
[184] R.M. López, V.V. Spirin, S.V. Miridonov, M.G. Shlyagin, G. Beltran, E.A. Kuzin, Fiber optic distributed sensor for hydrocarbon leak localization based on transmission/reflection measurement, Opt Laser. Technol. 34 (6) (2002 Sep 1) 465–469.
[185] V.V. Spirin, M.G. Shlyagin, S.V. Miridonov, P.L. Swart, Alarm-condition detection and localization using Rayleigh scattering for a fiber-optic bending sensor with an unmodulated light source, Opt Commun. 205 (1–3) (2002 Apr 15) 37–41.
[186] V.V. Spirin, Transmission-reflection analysis for localization of temporally successive multipoint perturbations in a distributed fiber-optic loss sensor based on Rayleigh backscattering, Appl. Opt. 42 (7) (2003 Mar 1) 1175–1181.

[187] J. Li, J. Gan, Z. Zhang, X. Heng, C. Yang, Q. Qian, S. Xu, Z. Yang, High spatial resolution distributed fiber strain sensor based on phase-OFDR, Opt Express 25 (22) (2017 Oct 30) 27913–27922.
[188] M. Cen, V. Moeyaert, P. Mégret, M. Wuilpart, Localization and quantification of reflective events along an optical fiber using a bi-directional TRA technique, Opt Express 22 (8) (2014 Apr 21) 9839–9853.
[189] V.V. Spirin, F.J. Mendieta, S.V. Miridonov, M.G. Shlyagin, A.A. Chtcherbakov, P. L. Swart, Localization of a loss-inducing perturbation with variable accuracy along a test fiber using transmission-reflection analysis, IEEE Photon. Technol. Lett. 16 (2) (2004 Feb 19) 569–571.
[190] M. Silveira, A. Frizera, A. Leal-Junior, D. Ribeiro, C. Marques, W. Blanc, C.A. Diaz, Transmission–reflection analysis in high scattering optical fibers: a comparison with single-mode optical fiber, Opt. Fiber Technol. 58 (2020 Sep 1) 102303.
[191] L. Avellar, M. Silveira, C.A. Diaz, C. Marques, A. Frizera, W. Blanc, A. Leal-Junior, Transmission-reflection performance analysis using oxide nanoparticle-doped high scattering fibers, IEEE Photon. Technol. Lett. 34 (16) (2022 Jul 13) 874–877.
[192] L. Avellar, A. Frizera, H. Rocha, M. Silveira, C. Díaz, W. Blanc, C. Marques, A. Leal-Junior, Machine learning-based analysis of multiple simultaneous disturbances applied on a transmission-reflection analysis based distributed sensor using a nanoparticle-doped fiber, Photon. Res. 11 (3) (2023 Mar 1) 364–372.
[193] Y. Zhang, J. Zhou, Y. Zhang, D. Zhang, K.T. Yong, J. Xiong, Elastic fibers/fabrics for wearables and bioelectronics, Adv. Sci. 9 (35) (2022 Dec) 2203808.
[194] L.M. Avellar, A.G. Leal-Junior, C.A. Diaz, C. Marques, A. Frizera, POF smart carpet: a multiplexed polymer optical fiber-embedded smart carpet for gait analysis, Sensors 19 (15) (2019 Jul 31) 3356.
[195] A. Leal-Junior, L. Avellar, A. Frizera, C. Marques, Smart textiles for multimodal wearable sensing using highly stretchable multiplexed optical fiber system, Sci. Rep. 10 (1) (2020 Aug 17) 13867.
[196] A.G. Leal-Junior, D. Ribeiro, L.M. Avellar, M. Silveira, C.A. Díaz, A. Frizera-Neto, W. Blanc, E. Rocon, C. Marques, Wearable and fully-portable smart garment for mechanical perturbation detection with nanoparticles optical fibers, IEEE Sensor. J. 21 (3) (2020 Sep 15) 2995–3003.
[197] N. Ilmane, S. Croteau, C. Duclos, Quantifying dynamic and postural balance difficulty during gait perturbations using stabilizing/destabilizing forces, J. Biomech. 48 (3) (2015 Feb 5) 441–448.
[198] L. Romeo, A. Petitti, R. Marani, A. Milella, Internet of robotic things in smart domains: applications and challenges, Sensors 20 (12) (2020 Jun 12) 3355.
[199] V.T. Tran, C. Riveros, P. Ravaud, Patients' views of wearable devices and AI in healthcare: findings from the ComPaRe e-cohort, NPJ Dig. Med. 2 (1) (2019 Jun 14) 53.
[200] A. Leal-Junior, L. Avellar, W. Blanc, A. Frizera, C. Marques, Opto-electronic smart home: heterogeneous optical sensors approaches and artificial intelligence for novel paradigms in remote monitoring, IEEE Internet Things J. (2023 Oct 10).
[201] H. Cao, A.P. Mosk, S. Rotter, Shaping the propagation of light in complex media, Nat. Phys. 18 (9) (2022 Sep) 994–1007.
[202] Colliard L, Aubry G, Cabié M, Neisius T, Pigeonneau F, Vallée R, Bernier M, Bellec M, Blanc W. Femtosecond laser tuning of nanoparticles in optical fibers. 2024. Proc. SPIE PC12142, Fiber Lasers Glass Photon.: Mater. Appl. III.
[203] J.W. Arkwright, I.D. Underhill, S.A. Maunder, N. Blenman, M.M. Szczesniak, L. Wiklendt, I.J. Cook, D.Z. Lubowski, P.G. Dinning, Design of a high-sensor count fibre optic manometry catheter for in-vivo colonic diagnostics, Opt Express 17 (25) (2009 Dec 7) 22423–22431.
[204] F. Khan, A. Denasi, D. Barrera, J. Madrigal, S. Sales, S. Misra, Multi-core optical fibers with Bragg gratings as shape sensor for flexible medical instruments, IEEE Sensor. J. 19 (14) (2019 Mar 14) 5878–5884.